This document is currently under revision by the European Commission (EC) and has not yet been validated or approved by the EC. The content provided herein is subject to change, and the information presented may not represent the final position or official stance of the EC.

This document is being shared for informational purposes only and is not to be considered an official or authoritative source of information from the European Commission. Any decisions, actions, or interpretations based on the content of this document should be taken with caution, as the content may be subject to modification or revision by the EC.

The EC accepts no liability for any inaccuracies, errors, or omissions in this document, and any reliance on its content is at the user's own risk. It is recommended to verify the information provided in this document with official EC publications or communications before making any decisions or drawing any conclusions based on its content.

Please note that the content in this document may be confidential or sensitive in nature and should be treated as such. Unauthorized dissemination, distribution, or use of this document is strictly prohibited.

By accessing and reviewing this document, you acknowledge and accept the terms of this disclaimer.

BL2F

Transforming Black Liquor to Biofuel

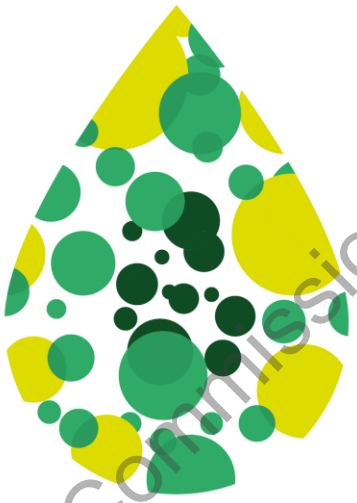

Research and Innovation Action

H2020-LC-SC3-2019-NZE-RES-CC

Process design and analysis of the integration of the production of HTL biofuels in conventional pulp mills

WP4 - Task 4.1

Date [M30]

Lead Beneficiary: TAU

Author(s): Vaibhav Agrawal (TAU), Gonzalo del Alamo (SINTEF-ER), Thomas Indlekofer (SINTEF-ER), Lotta Sorsamäki (VTT)

@BL2F_EU

www.bl2f.eu

BL2F_EU

Disclaimer

The content of this deliverable reflects only the author's view. The European Commission is not responsible for any use that may be made of the information it contains.

This project has received funding from the European Union's Horizon 2020 research and innovation programme under the Grant Agreement n°884111.

Document Information

Grant agreement	884111
Project title	Black Liquor to Fuel by Efficient Hydrothermal Application integrated to Pulp Mill
Project acronym	BL2F
Project coordinator	Prof. Dr. Tero Joronen
Project duration	1st April 2020 – 30th September 2023 (42 Months)
Related work package	WP 4 -Techno-economic assessment
Related task(s)	Task 4.1 – Integrated process analysis
Lead organisation	TAU
Contributing partner(s)	TAU, SINTEF-ER, VTT
Due date	30. 09. 2022 (M30)
Submission date	31. 10. 2022 (M31)
Dissemination level	Public

History

Date	Version	Submitted by	Reviewed by	Comments
27/10/2022	N°1	TAU	Tero Joronen	

Table of contents

List of figures

List of tables

Abbreviations and acronyms

Acronym	Description
WP	Work Package
BL	Black liquor
IHTL	Integrated Hydrothermal Liquefaction
APR	Aqueous phase reforming
IHDO	Integrated Hydrodeoxygenation
adt	air dry ton

Executive Summary

BL2F aims to produce biofuel from the Black Liquor (BL) by developing Hydrothermal Liquefaction (HTL) technology. To improve the economics of the produced biofuel, two integration is conceptualized in BL2F - (1) integration of salt separation and HTL reaction in a novel Integrated Hydrothermal Liquefaction, (IHTL), reactor, and (2) integration of complete HTL process with traditional kraft pulp mill. In the second integration, BL will be taken from pulp mill to HTL plant and all side streams of the HTL plant will be recycled back to pulp mill. To study the technological challenge arising from these integrations, a detailed flow diagram of the HTL process, including the downstream processing such as Integrated Hydrodeoxygenation (IHDO) and Aqueous Phase Reforming (APR) is designed and presented in this report.

This deliverable reports the pre-commercial process design of the BL2F technological route for production of biofuel from black liquor at the pulp mill. The process design has been described through detailed process flow diagrams (PFDs) including all main processes and auxiliary equipment. Semi-empirical process models for the processes involved in the HTL plant and the upgrading of the HTL biocrude to biofuels has been developed and described in Sections 3 and 5. These models include empirical parameters, evaluated from experiments results, to evaluate the total mass and energy balances for each of the processes involved in the overall conversion from black liquor to biofuels. Preliminary calculation of the process for the HTL plant shows mass and energy yields of biocrude relative to the black liquor feed of approximately 16% and 42% respectively. The yields for naphtha, kerosene, and diesel relative to the biocrude feed into the upgrading are 24.2%, 20.1% and 34.3% on dry mass basis and 27%, 22% and 39% on chemical energy basis, respectively.

Analysis of the integration of HTL process with pulp mill is also described in this report. The flow calculations obtained from the process analysis of the HTL plant have been used as interface with a process model of the pulp mill implemented in WinGEMS tool to evaluate the impact of integrating the HTL plant into the pulp mill. Three different scenarios were simulated depending on the amount of weak BL directed to the HTL process. In BL2F5, BL2F10 and BL2F30 scenarios, 5, 10 or 30% of weak BL was directed to HTL plant, respectively. The results from these BL2F scenarios are compared with the reference pulp mill model, in which no BL is extracted from pulp mill.

As expected, taking part of weak BL to HTL process reduces the thermal capacity of the recovery boiler and consequently the electricity production of the turbine plant. The thermal capacity of the recovery boiler decreases by 3, 6 or 17% when 5, 10 or 30% of black liquor is taken to HTL plant, respectively. The net electricity production decreases by 11, 23 or 69% respectively for BL2F5, BL2F10, BL2F30 compared to reference case. However, in all evaluated BL2F scenarios, the pulp mill is still self-sufficient regarding its steam and electricity consumption. Also, there is enough heat available for the HTL plant. The evaporation capacity reduces by 1%, 2% and 5% in BL2F5, BL2F10 and BLF30 scenarios as lesser BL is available for evaporation. From the detailed analysis of the recycling of cooking chemicals back to pulp mill, 7%, 15% and 44% of additional sodium is required in BL2F5, BL2F10 and BL2F30 scenarios while negligible amount of additional sulfur is required in any BL2F scenarios. The integration of the HTL plant has a negligible effect on pulp mill's freshwater consumption or wastewater production.

Keywords

Black liquor, HTL, integration, pulp mill, process simulation, Fuel, Aviation, Shipping

1 Introduction

1.1 Purpose of this deliverable

The primary objective of this deliverable is to define the process design and evaluate the process performance of the production of marine and aviation biofuels from black liquor based on the integration of hydrothermal liquefaction into a representative kraft pulp mill.

The specific objectives are:

1. Develop pre-commercial process flow diagrams of the integrated process design to include the main process and auxiliary equipment.
2. Specify the process design parameters of main technologies conforming the overall integrated process.
3. Develop semi-empirical process models for the HTL plant and the biocrude upgrading to calculate mass and energy flows based on experimental results.
4. Perform a preliminary process analysis of the HTL plant and its integration into the pulp mill, and of the upgrading of biocrude to biofuels.

1.2 Background information and input data from other tasks

The following information has been used (see also references):

1. General objectives, technological options and process performance targets from the proposal SEP-210593035, " Black Liquor to Fuel by Efficient HydroThermal Application integrated to Pulp Mill."

2. Measurements of the composition of black liquor samples. Reported in the deliverable H2020-LC-SC3-2019-NZE-RES-CC/D1.3, 2021, "Report on the feedstock characterization"

3. The description of a hardwood kraft pulp mill process model that forms the basis for the simulations studying the integration of the HTL plant into the pulp mill is presented in Kangas el at. 2014.

1.3 Symbology

The symbology used in HTL modelling are presented in Table 1.

Table 1: Symbology and Process performance targets

Symbol	Description
Variables	
$\dot{M}, \dot{V}, \dot{V}_N$	Mass flow rate, volumetric flow rate, normal volumetric flow rate
Y, X, ϕ	Mass fraction, mole fraction, volume fraction
$\dot{H}, \dot{H}_T, \dot{H}_F,$	Rate of total, thermal and formation enthalpy
$\dot{Q}, \dot{W}_{el}$	Heat power, electric power

h, h_T, h_F	Specific total, thermal and formation enthalpy per unit mass
$\bar{h}$, $\bar{h}_T$, $\bar{h}_F$	Specific total, thermal and formation enthalpy per unit mole
ρ, k, μ	Bulk density, thermal conductivity and viscosity
c, c_P	Specific heat, specific heat at constant pressure
Subscripts	
i	Atomic composition
j	Molecular composition
k (O, W, S, G)	Phase composition (oil, aqueous, solid and gas phases)
l	Biomass constituent or molecular functional group
bl	Black liquor
O	Oil phase
S	Solids phase, insoluble fraction
A	Aqueous phase, including solubilized material
G	Gas phase
cat	Catalyst
$solv$	Solvent
h	Heating
c	cooling
el	electricity
Superscripts	
F	Raw feedstock
SP	Salts precipitation
HTL	Hydrothermal liquefaction
IHDO	First-stage hydrodeoxygenation
PS	Phase separation
APR	Aqueous Phase Reforming
$HDTR$	Hydrotreating
$HDCR$	Hydrocracking
HDI	Hydro-isomerization

2 Process design

2.1 HTL plant design

The process design of the HTL plant is graphically represented through the process block diagram shown in Figure 1 and the process flow diagrams shown in Figure 14-Figure 19 in Annex A.

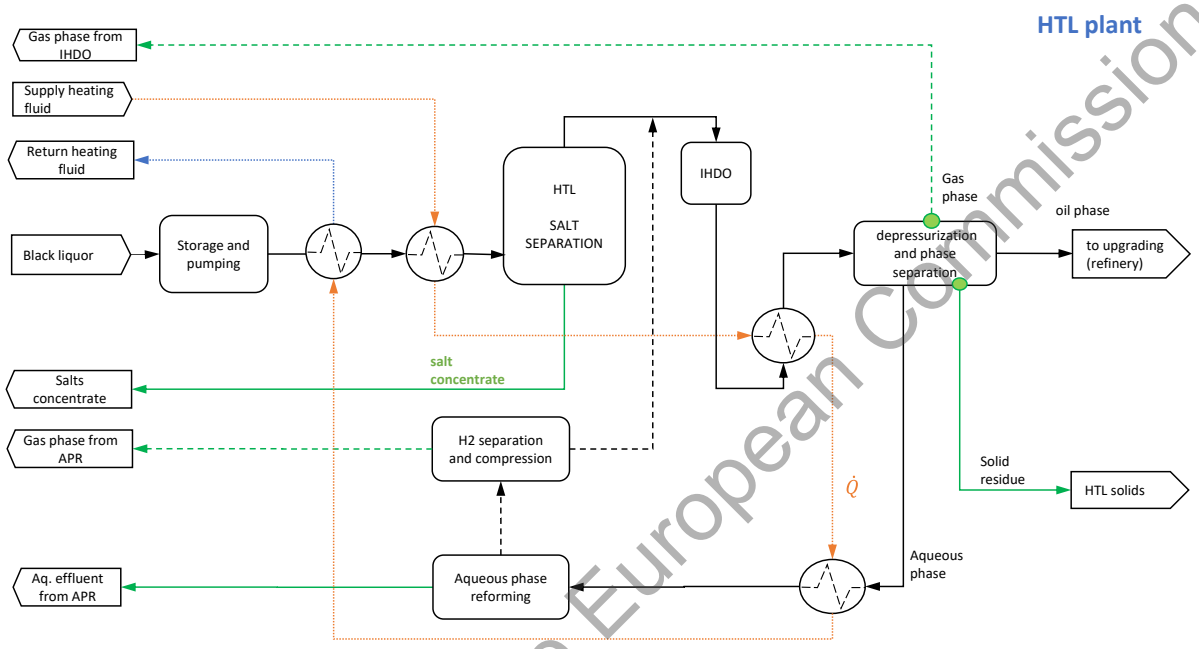

Figure 1: Process block diagram representing the process design of the HTL plant for production of bio-oil from black liquor.

2.1.1 Salt separation, liquefaction and first-stage hydrodeoxygenation

The process design is described through the process flow diagram shown in Figure 14 in Annex A. The black liquor is stored in a storage tank which is designed as a stirred tank coupled with heating jacket. Stirring ensures uniform mixing of the black liquor and heating jacket increases the temperature of the black liquor which reduces the viscosity and thus improves its pumpability. The back liquor is discharged from the storage tank by a pump that feeds the main pressurization pump which increases the pressure to supercritical-water conditions. The pressurization pump is designed as a single piston low stroke reciprocating pump. The pressurized slurry is heated to HTL conditions in a jacked U-tube heat exchanger in a controlled heating rate and then fed into the bottom of IHTL reactor. The process design considers one or several parallel HTL reactors depending on the capacity of the biocrude production plant. The HTL reactor is adiabatic and dimensioned to achieve the required residence time to complete the liquefaction of the slurry. The product from the HTL reactor is cooled down in a heat exchanger before undergoing depressurization. Heating of the slurry and cooling of the

HTL product is performed in a closed loop using a thermal fluid that recovers the heat from cooling of the HTL product.

2.1.2 Phase separation

The process design is described through the process flow diagram shown in Figure 15 in Annex A. HTL product obtained after cooling the outlet of the IHTL reactor is a mixture of different phases such as biocrude, hydrochar, and aqueous phase. This HTL product needs to be separated into constituent phases to characterize and analyze the properties of each phase. As a result, a novel phase separation process was developed at TAU. The process was developed using the HTL product received from SINTEF.

SINTEF conducted the experiments in their continuous HTL facility at temperature of 390 °C and pressure of 290-300 bar. 5 ml of Methyl Ethyl Ketone (MEK) was added to the 100 ml HTL product which facilitates the settling of the possible light biocrude onto the surface of the aqueous phase. HTL product was then centrifuged at 4500 rpm for 10 min. After centrifugation two distinguishable phases were formed. The upper phase is the aqueous phase, and the lower phase is the mixture of biocrude and hydrochar. The aqueous phase was transferred to a beaker and stored for analysis. The remaining lower phase was diluted with a fixed amount of Dichloromethane (DCM). The diluted mixture of biocrude and hydrochar was centrifuged again at 4500 rpm for 10 min. After second centrifugation, solids settled at the bottom of the centrifugation container. The upper phase which mostly contains diluted biocrude, was transferred to another centrifugation bottle and was centrifuged for third time at 4500 rpm for 10 min to remove all the possible solids. The DCM was recovered from the pure diluted biocrude (upper phase after the 3rd centrifugation) through a vacuum rotary evaporator operating at 60 °C and 56 KPa. The dense by-product left in the rotary flask is pure biocrude. The lower solid phase from second and third centrifugation were mixed and were analysed for hydrochar and impurities.

2.1.3 Aqueous Phase Reforming (APR)

The process design is described through the process flow diagram shown in Figure 16 in Annex A. HTL-oil aqueous stream can be converted into hydrogen by performing the aqueous phase reforming (APR) experiments. The efficiency of these experiments is, however, constrained by the hydrothermal and high-pressure operating conditions (Coronado et al., 2017). These conditions consequently limit the reaction kinetics, thermodynamics, and catalyst stability (Coronado et al., 2017). As a result, an active and durable catalyst needs to be developed to overcome these limitations.

As part of the AQUACAT project funded by the Academy of Finland, catalysts were developed to selectively convert the oxygenated hydrocarbons present in the aqueous stream into hydrogen. Out of the developed catalysts, 3-5 promising catalysts will be screened for the BL2F project by applying the real aqueous streams into the continuous laboratory scale APR facility at VTT. The continuous APR facility at VTT consists of an 8 mm (inner diameter) tubular stainless steel reactor. The catalysts are loaded into the reactor and the products obtained are first cooled in a heat exchanger and then separated into gas and liquid (Figure 2). The gas and the

liquid streams are then analysed by gas chromatography (GC) in an online and offline mode, respectively. The gases are analysed in an Agilent Technologies 490 Micro GC, whereas the liquid products are analysed in Shimadzu GC-2010 Plus equipped with an FID and a HP-INNOWax Polyethylene Glycol column.

Initial experiments will be performed with the feed mixtures simulating the real feed to accelerate the experimental work before switching to the real aqueous feed. The real feed will be obtained from the HTL experiments that will be performed at the Tampere University as part of the WP1. The emphasis of these experimental work will be on the long-term stability of catalysts, i.e., long-term experiments with model and real feed and different catalysts will be performed in practice. Fresh and spent catalysts will also be characterized. If required, a limited effort on the further development of the catalyst can be performed in the project to improve the stability of the most promising catalyst. Catalyst stability will be assessed for the presence of salts remaining in the aqueous feed after the IHTL experiments. The application of guard material will also be studied. Based on the results obtained from all the lab scale APR experiments, a concept for the (i) aqueous phase reforming integrated to pulp mill and (ii) hydrogen productivity by aqueous phase reforming will be developed.

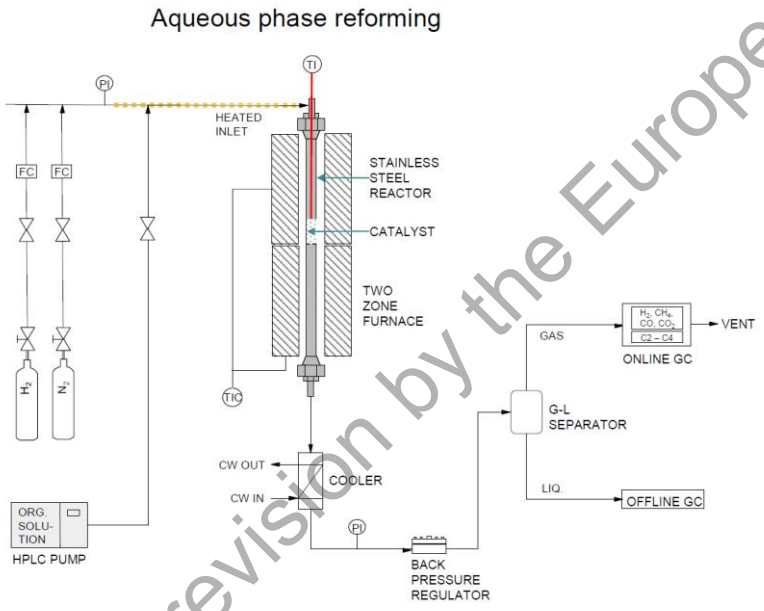

Figure 2 Continuous APR facility at VTT.

2.2 Kraft pulp mill process and integration of the HTL plant

The process block diagram in Figure 3 shows a schematic representation of kraft pulp mill process and the interfaces with the HTL plant. Part of the weak black liquor, having a dry matter content of approximately 15 wt%, is separated before evaporation and directed to HTL plant. Five side streams of the HTL plant are recycled back to the pulp mill. Aqueous effluent from APR is mixed with rest of the weak black liquor and directed to evaporation plant for concentration. Gas streams from both phase separation and APR are combined with other non-condensable gases from evaporation and treated in recovery boiler. Salt concentrate from salt

separation and solid fraction from phase separation are mixed with strong black liquor from evaporation and burned in the recovery boiler.

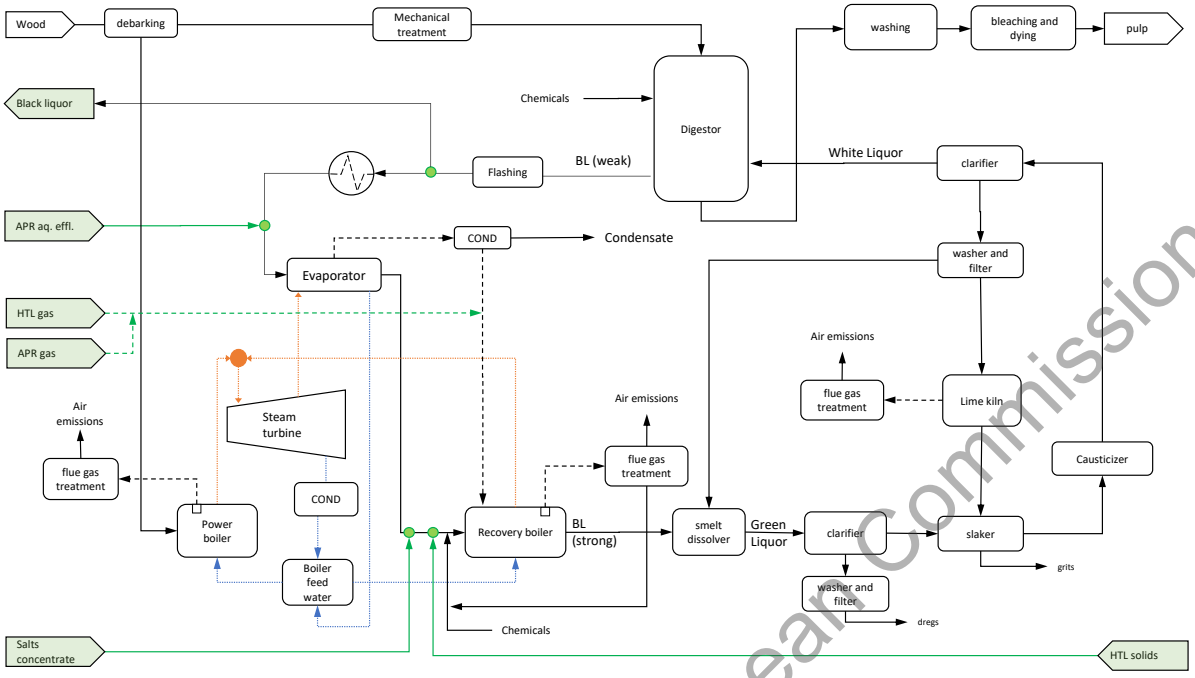

Figure 3: Process block diagram representing the kraft pulp mill with interfaces with the HTL plant

The integration modelling was conducted with WinGEMS steady-state process simulator. Three BL2F-scenarios were modelled and compared with the reference scenario. The reference scenario depicts the reference pulp mill which is a hardwood (birch) kraft pulp mill producing 100 adt pulp/h. The design of the reference pulp mill is described in detail by Kangas et al. (2014). In the BL2F-scenarios, 5%, 10% or 30% of weak black liquor before evaporation is separated and directed to the HTL plant. The composition of the black liquor is derived from the reference scenario modelling. The compositions and flows of the HTL side streams are derived from the HTL plant modelling.

The energy integration of the HTL plant to the pulp mill is implemented as follows. In the reference scenario, all fresh steam (103 bar, 505 °C) from recovery boiler is fed to turbine plant where required amounts of 30 bar (HP), 13 bar (MP) and 4.2 bar (LP) steam are produced to cover the pulp mill's own steam consumption. Surplus heat is used to produce electricity. Pulp mill's own electricity consumption is assumed to be 600 kWh/adt (60 MW). Surplus electricity is sold. In BL2F-scenarios, part of the fresh steam (103 bar and 505 °C) from recovery boiler is used in HTL plant for heating purposes. The estimate for the total heat demand of the HTL plant (0.118 MJ/kg BL) is derived from the HTL plant modelling. The condensate from the HTL plant is returned at 100 bar and 300 °C back to turbine plant. In BL2F-scenarios, rest of the fresh steam from recovery boiler is fed to turbine plant where required amounts of HP, MP and LP steam are produced to cover the pulp mill's own steam consumption. Surplus heat is used to produce electricity. Surplus electricity, after subtracting pulp mill's own electricity

consumption (60 MW), is available for HTL-plant's use or for sale. The electricity consumption of the HTL-plant is not included in the evaluation.

The effect of HTL integration on the reference pulp mill's energy, sodium and sulfur balances was evaluated by comparing the mass and energy balances of the evaluated concepts.

2.3 Upgrading of HTL oil to marine and aviation fuels

Figure 4 shows a schematic representation of the overall process for the upgrading of the biocrude produced from hydrothermal liquefaction to naphtha and diesel fractions for further used as marketable road fuels. More detailed flowsheets are presented in Figure 17-Figure 19. The main process steps include:

- Removal of inorganic heteroatoms in a catalytic guard reactor
- Catalytic hydrotreating of the biocrude for reduction of oxygen, sulfur, and nitrogen with hydrogen.
- Separation of the gas phase, water, and organic liquid from the hydrotreating and hydrocracking products.
- Fractionation of the liquid organic by distillation with production of naphtha, kerosene, and heavy distillate.
- Catalytic hydrocracking of the heavier fraction from distillation for further production of naphtha and kerosene. The product from hydrocracking is recirculated to the separation process after hydrotreating.
- Hydro-isomerization of the naphtha for production of kerosene.
- Treatment of the gas product from separation by removal of CO_2, NH_3 and H_2S and recirculation of purified hydrogen back to guard reactor, hydrotreater and hydrocracker.

The main products of the overall upgrading process considered in the analysis are kerosene, used as jet-fuel, and heavy distillate used as marine fuel. Naphtha is as an intermediate for producing gasoline via isomerization before being blended again in the gasoline pool at the refinery (C. U. Jensen, 2016)]. The middle distillate is assumed to be blended directly in the diesel pool at the refinery.

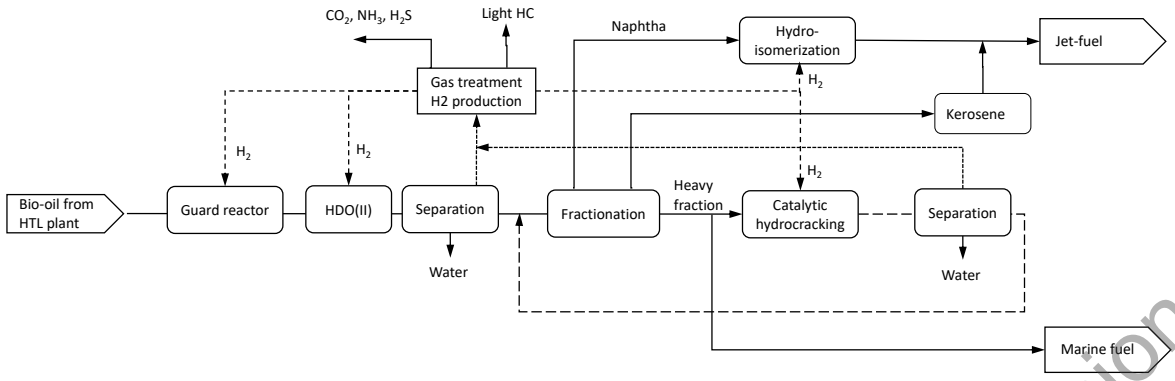

Figure 4: Process block diagram representing the upgrading of bio-oil derived from black liquor to aviation and marine fuels based on conventional refinery processes

3 HTL plant process modelling and analysis

3.1 HTL plant modelling

3.1.1 Black liquor characterization

The process analysis considers the reference black liquor composition shown in Table 5, which includes the dry matter content, high heating value, elementary composition, concentration of the main constituents, and chemical composition of the salts.

3.1.2 Salt separation

The salt separation process is calculated semi-empirically throughout the precipitation factor of each salt species j dissolved in the aqueous phase, denoted by η_j^{PREC}. From this definition, the mass flow rates flow rates of the solid and the liquid phases of the precipitated salts brine are calculated from

$$\begin{bmatrix} \dot{M}_S^{PREP} \\ \dot{M}_L^{PREP} \end{bmatrix} = \dot{M}_{bl}^{HTL} \begin{bmatrix} Y_L^F \sum_j Y_{L,j}^F \eta_j^{PREC} + \eta_L^{PREC} Y_S^F \\ Y_L^F \sum_j Y_{L,j}^F \left(1 - \eta_j^{PREC}\right) \eta_L^{PREC} \end{bmatrix}. \quad (1)$$

Here η_L^{PREC} represents the fraction of the liquid phase lost during extraction of the precipitated salts from the reactor, assumed to be constant and equal to 0.1. Here, the concentration of non-dissolved organics in the liquid phase that leaves the reactor with the precipitated solids is the same as for the black liquor. Under this assumption, the moisture content of the salts brine is calculated from

$$Y_{H2O}^{PREC} = \left(\eta_L^{PREC} Y_{H_2O}^F\right) / \left[Y_L^F \sum_j Y_{L,j}^F \left(\eta_j^{PREC} + \left(1 - \eta_j^{PREC}\right) \eta_L^{PREC}\right) + \eta_L^{PREC} Y_S^F\right].$$

Preliminary values of the salt precipitation factors are shown in Table 2 based on experimental results on model compounds reported by PSI.

Table 2**:** Preliminary values of the salt precipitation factors used in the analysis

Salt	Precipitation factor
NaOH	1.00
NaHS	0.93
Na_2SO_4	0.89
$Na_2S_2O_3$	0.80
Na_2CO_3	0.98
K_2CO_3	1.00

The mass flow rates of the slurry product and the solids and liquid phases leaving the salt separation and entering the HTL process is calculated from

$$\dot{M}_{SL}^{HTL} = \dot{M}_{bl}^{HTL} \left[Y_L^F \sum_j Y_{L,j}^F \left(1 - \eta_j^{PREC}\right) + Y_S^F\right] \left(1 - \eta_L^{PREC}\right) \text{ and}$$

$$\begin{bmatrix} \dot{M}_S^{HTL} \\ \dot{M}_L^{HTL} \end{bmatrix} = \dot{M}_{bl}^{HTL} \begin{bmatrix} \left(1 - \eta_L^{PREC}\right) Y_S^F \\ Y_L^F \sum_j Y_{L,j}^F \left(1 - \eta_j^{PREC}\right) \left(1 - \eta_L^{PREC}\right) \end{bmatrix}. \quad (2)$$

Neglecting the calorific value of the salts, the rate of chemical enthalpy from the salts brine and slurry product from salt separation are calculated from $\dot{H}_{SL}^{PREC} = \dot{M}_{bl}^{HTL}[\eta_L^{PREC} Y_S^F HHV_S^F]$ and $\dot{H}_{SL}^{PREC} = \dot{M}_{bl}^{HTL}[(1-\eta_L^{PREC}) Y_S^F HHV_S^F]$.

3.1.3 Hydrothermal liquefaction process

The overall conversion of the slurry in the hydrothermal liquefaction process has been evaluated semi-empirically throughout the so-called transfer coefficients $\eta_{i,k}^{HTL}$ and $\eta_{H_c,k}^{HTL}$ defined, respectively, as the distribution of the atomic mass and chemical enthalpy of the dry fraction of the input slurry among the different phases produced from the hydrothermal liquefaction process. Here the subscript k denotes the oil (O), gas (G), solid (S) and aqueous (A) phases, and the subscript i denotes an atomic element. From these definitions, the mass flow rates, dry atomic composition, and enthalpy flow rates of the product phases after the HTL process are calculated from

$$\begin{bmatrix} \dot{M}_O^{HTL} \\ \dot{M}_A^{HTL} \\ \dot{M}_S^{HTL} \\ \dot{M}_G^{HTL} \end{bmatrix} = \dot{M}_{bl}^{SS} \begin{bmatrix} Y_S^{HTL} \sum_i Y_{S,i}^{HTL} \eta_{i,O}^{HTL} \\ Y_L^{HTL} + Y_S^{HTL} \sum_i Y_{S,i}^{HTL} \eta_{i,A}^{HTL} \\ Y_S^{HTL} \sum_i Y_{S,i}^{HTL} \left(1 - \eta_{i,O}^{HTL} - \eta_{i,A}^{HTL} - \eta_{i,G}^{HTL}\right) \\ Y_S^{HTL} \sum_i Y_{S,i}^{HTL} \eta_{i,G}^{HTL} \end{bmatrix} \quad (3)$$

$Y_{i,k}^{HTL} = \left(Y_{S,i}^{HTL} \eta_{k,i}^{HTL}\right) / \sum_i Y_{S,i}^{HTL} \eta_{k,i}^{HTL}$ and $\dot{H}_{c,k}^{HTL} = \dot{M}_S^{HTL} HHV_S^{HTL} \eta_{H_c,k}^{HTL}$.

Here, it has been assumed that the dissolved components in water remain unreacted during conversion in the liquefaction process. Table 3 shows preliminary values of the transfer coefficients $\eta_{i,k}^{HTL}$ and $\eta_{H_c,k}^{HTL}$ used in the analysis reported in this document.

Table 3: Estimated transfer coefficients for the mass distribution of the main atomic elements and chemical enthalpy contained in the black liquor among the oil, aqueous, solid and gas product phases in the hydrothermal liquefaction process.

	Oil phase (%)	Aqueous phase (%)	Solid phase (%)	Gas phase (%)
Chemical enthalpy	51.9	37.5	5.1	5.5
Carbon, C	50.0	24.0	6.0	20
Hydrogen, H	38.0	40.0	16.0	6
Oxygen O	4.1	44.0	19.9	32
Nitrogen N	14.0	58.0	16.0	12
Sulfur, S	14.0	18.0	13.0	55
Phosphorous, P	0.5	7.5	92.0	3.1
Calcium, Ca	0.0	6.0	94.0	0.0
Aluminium, Al	2.5	11.0	86.5	0.0
Iron, Fe	1.4	4.0	94.6	0.0
Magnesium, Mg	0.1	2.0	97.9	0.0
Potassium, K	2.0	75.1	22.9	0.0
Chlorine, Cl	0.0	37.0	63.0	0.0
Sodium, Na	4.2	54.5	41.3	0.0
Silicon, Si	10.0	3.4	86.6	0.0
Manganese, Mn	0.0	5.5	94.5	0.0

3.1.4 First-stage hydrodeoxygenation

The overall process in the IHDO is defined in terms of the yields y_K^{IHDO} and composition $y_{i,k}^{IHDO}$ of the oil, gas and aqueous phases at the reactor outlet and the required input hydrogen $\dot{M}_{H_2}^{IHDO}$. Here, the subscripts k denote the oil (O), gas (G) and aqueous (A) phases, and the subscript i denotes the atomic composition. The input hydrogen is calculated from

$$\dot{M}_{H_2}^{IHDO} = \dot{M}_f^{IHDO} y_O^{HTL} m_{H_2,r}^{IHDO} \lambda_{H_2}^{IHDO},$$

where $m_{H_2,r}^{IHDO}$ denote the hydrogen reacted per unit mass of input feed and $\lambda_{H_2}^{S}$ is the ratio between the total hydrogen input and the reacted hydrogen. The reaction hydrogen consumption has been estimated based on the atomic composition of S and O heteroatoms. From these definitions, the mass flow rate of the oil, gas, and aqueous phases are calculated from

$$\begin{bmatrix} \dot{M}_O^{IHDO} \\ \dot{M}_A^{IHDO} \\ \dot{M}_G^{IHDO} \\ \dot{M}_S^{IHDO} \end{bmatrix} = \begin{bmatrix} \dot{M}_O^{HTL} \\ \dot{M}_A^{HTL} \\ \dot{M}_G^{HTL} \\ \dot{M}_S^{HTL} \end{bmatrix} + \dot{M}_O^{HTL} \left\{ \sum_i Y_{O,i}^{HTL} \begin{bmatrix} \eta_{i,O}^{IHDO} \\ \eta_{i,A}^{IHDO} \\ \eta_{i,G}^{IHDO} \\ 0 \end{bmatrix} + m_{H_2,r}^{IHDO} \begin{bmatrix} \eta_{H_2,O}^{IHDO} \\ \eta_{H_2,A}^{IHDO} \\ \eta_{H_2,G}^{IHDO} + \left(\lambda_{H_2}^{IHDO} - 1\right) \\ 0 \end{bmatrix} \right\} \quad (4)$$

It is assumed that the only hydrogen stream available for IHDO is the one produced from the aqueous phase reforming system. Similarly, the atomic composition can be evaluated from

$$\left\{ \begin{array}{c} Y_{i,k}^{IHDO} = \left(Y_{f,i}^{IHDO} \eta_{i,k}^{IHDO}\right) / \left[m_{H_2,r}^{IHDO} \eta_{H_2,K}^{IHDO} + \sum_i Y_{f,i}^{IHDO} \eta_{i,k}^{IHDO}\right] \text{ for } i \neq H \text{ and } k \neq G \\ Y_{i,k}^{IHDO} = \left(Y_{f,i}^{IHDO} \eta_{i,k}^{IHDO} + m_{H_2,r}^{IHDO} \eta_{H_2,K}^{IHDO}\right) / \left[m_{H_2,r}^{IHDO} \eta_{H_2,K}^{IHDO} + \sum_i Y_{f,i}^{IHDO} \eta_{i,k}^{IHDO}\right] \text{ for } i = H \text{ and } k \neq G \\ Y_{i,G}^{IHDO} = \left(Y_{f,i}^{IHDO} \eta_{i,G}^{IHDO}\right) / \left[m_{H_2,r}^{IHDO} \left(\eta_{H_2,G}^{IHDO} + \lambda_{H_2}^{IHDO} - 1\right) + \sum_i Y_{f,i}^{IHDO} \eta_{i,G}^{IHDO}\right] \text{ for } i \neq H \\ Y_{H,G}^{IHDO} = \left(Y_{f,i}^{IHDO} \eta_{i,G}^{IHDO} m_{H_2,r}^{IHDO} \left(\eta_{H_2,G}^{IHDO} + \lambda_{H_2}^{IHDO} - 1\right)\right) / \left[m_{H_2,r}^{IHDO} \left(\eta_{H_2,G}^{IHDO} + \lambda_{H_2}^{IHDO} - 1\right) + \sum_i Y_{f,i}^{IHDO} \eta_{i,G}^{IHDO}\right] \end{array} \right\} \quad (5)$$

Preliminary values for the coefficients $\eta_{i,K}^{IHDO}$, $\eta_{H_2,K}^{IHDO}$, with $K = O, A, G$ denoting the oil, aqueous and gas phases, are shown in Table 4.

Table 4: Estimated values of the transfer coefficients for dry atomic composition of the feed $\eta_{i,k}^{IHDO}$ and the reacted hydrogen $\eta_{H_2,k}^{IHDO}$ among product phases in the IHDO process.

Phase	Oil	Gas	Aqueous
Reacted H2	0.70	0.21	0.09
C (dry feed)	0.899	0.006	0.096
H (dry feed)	0.924	0.007	0.069
O (dry feed)	0.656	0.005	0.338
S (dry feed)	0.231	0.128	0.641

3.1.5 Phase separation

The mass flow rates, dry atomic composition and enthalpy flow rates of the oil, solid, aqueous and gas phases after phase separation are calculated from

$$\begin{bmatrix} \dot{M}_O^{PS} \\ \dot{M}_A^{PS} \\ \dot{M}_S^{PS} \\ \dot{M}_G^{PS} \end{bmatrix} = \dot{M}_{bl}^{SS} \begin{bmatrix} \dot{M}_O^{IHDO} \eta_{A,O}^{PS} \\ \dot{M}_A^{IHDO} \left(1 - \eta_{A,O}^{PS} - \eta_{A,S}^{PS}\right) \\ \dot{M}_S^{IHDO} \eta_{A,S}^{PS} \\ \dot{M}_G^{IHDO} \end{bmatrix}, \quad (6)$$

$Y_{i,k}^{HTL} = \left(Y_{F,i}^{HTL} f_{M,k,i}^{HTL}\right) / \sum_i Y_{F,i}^{HTL} f_{M,k,i}^{HTL}$ and $\dot{H}_{f,k}^{HTL} = \dot{M}_F^{HTL} Y_{F,DM}^{HTL} HHV_{F,DM}^{HTL} f_{H,k}^{HTL}$.

Here, the parameters $\eta_{A,O}^{HTL}$ and $\eta_{A,S}^{HTL}$ denote, respectively, the fraction of the aqueous phase present in the oil and the solids after the phase separation system. Preliminary calculations of these coefficients have been performed assuming a water content in the oil and solid phases of 1.5%wt and 23%wt respectively.

3.1.6 Aqueous Phase Reforming

The Aqueous Phase Reforming (APR) process has been evaluated in terms of the mass flow rates and composition of the gas and aqueous phase products. The mass flow rates are calculated from

$$\begin{bmatrix} \dot{M}_G^{APR} \\ \dot{M}_L^{APR} \end{bmatrix} = \dot{M}_A^{PS} \begin{bmatrix} \left(1 - y_{A,H_2O}^{PS}\right) \eta_g^{APR} \\ y_{A,H_2O}^{PS} + \left(1 - y_{A,H_2O}^{PS}\right)\left(1 - \eta_g^{APR}\right) \end{bmatrix}. \quad (7)$$

where the parameter η_g^{APR} representing the overall mass transfer to the gas phase in the APR process, which is calculated as the sum of the contribution from all molecular species j present in the feed aqueous solution that are reformed from $\eta_G^{APR} = \sum_j Y_{A,j}^{PS} \eta_{g,j}^{APR}$. The composition of the gas phase is calculated in terms of the mole fractions of species from

$$X_{G,k}^{APR} = \left[\sum_j \left(Y_{A,j}^{SEP} / MW_j\right) \eta_{g,j}^{APR} \chi_{j,k}^{APR}\right] / \eta_g^{APR},$$

with $\chi_{j,k}^{APR}$ denoting the selectivity of the gas species k from reforming of the aqueous species j. The composition of the aqueous phase product is then calculated performing a balance of the atomic mass.

3.2 Results from the HTL plant process analysis

3.2.1 Mass and energy flows

Annex B shows the calculated material and energy flows of the HTL plant based on the black liquor characterization and process parameters shown in Table 5 and Table 6. The dry mass and energy yields for the input and output flows of the HTL plant are shown in Table 6 and Table 8. The oil product contains approximately 16% and 42% of the dry mass and chemical energy, respectively, relative to the black liquor.

Table 5: Representative range of elementary composition of black liquor

Dry matter, DM (%wt)	15.8
HHV (MJ/kg) (dry basis)	13.3
Elemental analysis	
Carbon, C (%wt dry)	33.89
Hydrogen, H (%wt dry)	4.13
Oxygen, O (%wt dry)	31.07
Nitrogen, N (%wt dry)	0.00
Sulfur, S (%wt dry)	6.13
Phosphorous, P (g/kg dry)	0.05
Calcium, Ca (g/kg dry)	
Aluminium, Al (g/kg dry)	0.01
Iron, Fe (g/kg dry)	
Magnesium, Mg (g/kg dry)	0.30
Potassium, K (g/kg dry)	37.29
Chlorine, Cl (g/kg dry)	0.48
Sodium, Na (g/kg dry)	209.57
Silicon, Si (g/kg dry)	0.02
Manganese, Mn (mg/kg dry)	91
Composition of constituents	
Dissolved cellulose (%wt dry)	8.24
Dissolved hemicellulose (%wt dry)	21.64
Dissolved lignin (%wt dry)	30.49
Dissolved extractives (%wt dry)	1.35
Salts (%wt dry)	*24.7*
Composition of salts	
NaOH (%wt dry)	5.91
Na_2S (%wt dry)	0
NaHS (%wt dry)	9.44
Na_2SO_4 (%wt dry)	2.75
Na_2SO_3 (%wt dry)	0
$Na_2S_2O_3$ (%wt dry)	0.29
Na_2CO_3 (%wt dry)	3.36
K_2CO_3 (%wt dry)	2.92

Table 6: Process design parameters for the HTL plant

Process Parameter	Value
Black liquor feed temperature (°C) [a]	105
Black liquor feed pressure (bar-a)	1.01
Black liquor dry matter content (%wt)	15.8
Temperature at salt precipitation (°C)	350
Pressure at salt precipitation (bar-g)	320
Salts brine temperature (°C)	105
Salts brine pressure (bar-g)	2.0
Temperature at HTL (°C)	350
Pressure at HTL (bar-g)	320
IHDO temperature (°C)	350
IHDO pressure (bar-g)	320
Gravimetric separation temperature (°C)	150
Gravimetric separation pressure (bar-g)	30
Temperature at aqueous phase reforming (°C)	275
Pressure at aqueous phase reforming (bar-a)	30
Thermal fluid	Thermal oil
Thermal fluid supply temperature (°C)	400
Thermal fluid supply pressure (bar-g)	15

Table 7: Main dry mass yields for the HTL plant

Black liquor	Dry kg/s	1.000
Salt brine	Dry kg/s	0.312
Solid residue from phase separation	Dry kg/s	0.143
Liquid effluent from Aqueous Phase Reforming	Dry kg/s	0.210
Gas from phase separation	Dry kg/s	0.140
Gas from aqueous phase reforming	Dry kg/s	0.043
Oil product after phase separation	Dry kg/s	0.158

Table 8: Main energy yields for the HTL plant

Black liquor	MJ/s	1.000
Salt brine	MJ/s	0.100
Solid residue from phase separation	MJ/s	0.083
Liquid effluent from Aqueous Phase Reforming	MJ/s	0.306
Gas from phase separation	MJ/s	0,146
Gas from aqueous phase reforming	MJ/s	0.024
Oil product after phase separation	MJ/s	0.424
Thermal energy demand	MJ/s	0.056

4 Analysis of the integration of the HTL plant into the pulp mill

4.1 Approach of integration modelling

The integration modelling study was conducted with WinGEMS steady-state process simulator. The approach of the integration modelling was as follows:

1. Simulation of the reference scenario, i.e., the reference pulp mill
   - A previously created and documented simulation model will be used
2. Gathering data on the HTL streams and integration
   - Compositions of the recycled HTL side streams
   - Describing the HTL streams with available WinGEMS model components
3. Modification of the reference simulation model
   - Adding the uptake of black liquor and high-pressure steam
   - Adding the return of HTL side streams and condensate
4. Simulation of the BL2F-scenarios
   - BL2F5: 5% of weak black liquor taken to HTL plant
   - BL2F10: 10% of weak black liquor taken to HTL plant
   - BL2F30: 30% of weak black liquor taken to HTL plant
5. Comparison of the scenarios
   - Energy balances, sodium and sulfur balances

4.1.1 Simulation of the reference pulp mill

First the reference pulp mill was simulated. The design and the parameterization of the reference model is presented in Kangas et al. (2014). Mass and energy balances of the reference pulp mill were stored in an Excel-spreadsheet for further analysis and comparison. The mass and energy balances of the reference scenario serve as the basis, and the BL2F-scenarios will be compared to them.

4.1.2 Gathering data on the HTL streams and integration

The elementary (C, H, O, S, Na, Cl, K amounts) and salt (NaOH, NaHS, Na_2SO_4, $Na_2S_2O_3$, Na_2CO_3, K_2CO_3) compositions of the HTL streams resulted from HTL plant modelling are presented in Table 16 and Table 17 in Annex B; black liquor (flow #1), salt concentrate (#4), HTL solids (#8), APR aqueous phase (#12), APR gas (#14) and HTL gas (#15).

To be able to integrate the HTL side streams back to pulp mill simulation model, their elementary and salt compositions must be expressed in the WinGEMS model by using the following WinGEMS components:

- Organic components, with concentration of C, H, O and high heating values shown below.

	wt% C	wt% H	wt% O	HHV (MJ/kg dry)
Dissolved cellulose	46	6	48	17.6
Dissolved hemicellulose	46	6	48	17.6
Dissolved lignin	60	6	34	24.7
Dissolved extractives	77	12	11	37.0

- C, H and O also present in: hydroxide OH^- and carbonate CO_3^{2-}
- Sulfur components: sulfate SO_4^{2-}, hydrosulfide HS^- and thisulfate $S_2O_3^{2-}$
- Other ions: sodium (Na), chloride (Cl) and potassium (K)

The enthalpy content of the HTL streams recycled back to the pulp mill affects the pulp mill's recovery boiler thermal capacity. The sodium and sulfur contents of the HTL streams, on the other hand, affect the pulp mill's chemical balance, and thus the amount of cooking chemical makeup needs. When the elementary and salt compositions of the HTL streams were expressed with WinGEMS components, special attention was paid on the chemical enthalpy, sodium and sulfur contents. Table 9 presents the compositions (as wt% dry) of the HTL streams given in WinGEMS components. Table 10 shows how well the measured stream compositions from HTL plant modelling and the modelled stream compositions from WinGEMS process modelling correspond. Since the organic matter in the streams must be presented only with four WinGEMS components having fixed C/H/O-ratios, the measured (presented in Table 16 and Table 17 in Annex B) and modelled absolute amounts of carbon, hydrogen and oxygen were not consistent for HTL solids and APR aqueous effluent. However, this will not affect the enthalpy calculation in WinGEMS since the higher heating value (HHV) of the stream is calculated based on the HHVs of the organic components (dissolved cellulose/hemicellulose/lignin/extractives), and not based on the C/H/O contents. The measured higher heating value of the HTL solids fraction was not able to be reached with the available WinGEMS organic components and their HHVs. The actual enthalpy content of stream was, however, reached by adjusting both dry matter content and HHV of the stream. For HTL gas and APR gas, which are burned in the recovery boiler, WinGEMS calculates the heating value based on the C, H and O contents. Thus, HTL and APR gases were modelled in WinGEMS using their measured elementary compositions.

Table 9. The compositions (wt% dry) of HTL plant streams presented using WinGEMS components.

wt%	**Black liquor**	**Salt concentrate**	**HTL solids**	**APR aq. effluent**
Dissolved cellulose	8.24%	8.93%	53.54%	0%
Dissolved hemicellulose	21.64%	0%	0%	0%

Dissolved lignin	30.49%	10.89%	0%	41.49%
Dissolved extractives	1.35%	0%	0%	24.79%
Sodium	21.17%	33.50%	40.83%	25.25%
Sulfate	1.86%	5.37%	0.16%	0.79%
Thiosulfate	0.20%	0.53%	0.03%	0.16%
Hydrosulfide	5.57%	16.72%	0.30%	1.50%
Carbonate	3.17%	10.04%	0.03%	0.14%
Hydroxide	2.51%	8.05%	0%	0%
Potassium	3.75%	5.95%	4.87%	6.02%
Chloride	0.05%	0.02%	0.25%	0.07%

Table 10 The correspondence of the measured (HTL plant modelling) and the modelled (WinGEMS process modelling) stream compositions for HTL streams.

	Black liquor			**Salt concentrate**			**HTL solids**			**APR aq. effluent**		
	Model	Measur.	Error	Model	Measur.	Error	Model	Measur.	Error	Model	Measur.	Error
Dry matter, (kg/t)	158.31	158.40	0.1%	369.39	369.39	0.0%	187.72	229.55	18.2%	46.40	46.40	0.0%
HHV, (MJ/kg dry)	13.28	13.28	0.0%	4.26	4.26	0.0%	9.41	7.70	22.2%	19.37	19.37	0.0%
Chemical enthalpy (MW)	2.10	2.10	0.0%	0.21	0.21	0.0%	0.17	0.17	0.0%	0.64	0.64	0.0%
Carbon, C (kg/t)	53.48	53.49	0.0%	46.83	46.77	0.1%	46.24	42.71	8.3%	20.42	14.28	43.0%
Hydrogen, H (kg/t)	6.52	6.51	0.1%	8.07	8.13	0.8%	6.05	11.20	46.0%	2.51	1.99	26.1%
Oxygen, O (kg/t)	49.07	49.12	0.1%	101.08	101.09	0.0%	48.51	88.05	44.9%	8.10	14.75	45.1%
Sulfur, S (kg/t)	9.72	9.66	0.6%	67.61	67.54	0.1%	0.68	0.68	0.0%	0.84	0.84	0.1%
Sodium, Na (kg/t)	33.52	33.52	0.0%	123.76	123.76	0.0%	76.65	76.65	0.0%	11.71	11.71	0.0%

4.1.3 Modification of the reference simulation model

Figure 5 shows the overall flowsheet of the WinGEMS kraft pulp mill simulation model. Modification in the model were done in the Evaporation, Boiler plant and Turbine plant blocks marked with red rectangles. Figure 6 show print screen of Evaporation block with interfaces with the HTL plant. Part (5%/10%/30%) of weak black liquor is directed to HTL plant. Rest of it is mixed with APR aqueous effluent and directed to evaporation. The gas streams from HTL plant are mixed and burned in the recovery boiler together with bark pyrolysis gases. The HTL solids and salt concentrate are mixed with strong black liquor from evaporation and directed to recovery boiler for burning. The recycling of HTL streams dilute both the feed to evaporation and to recovery boiler. Figure 7 shows how the interfaces of HTL streams to Recovery plant block.

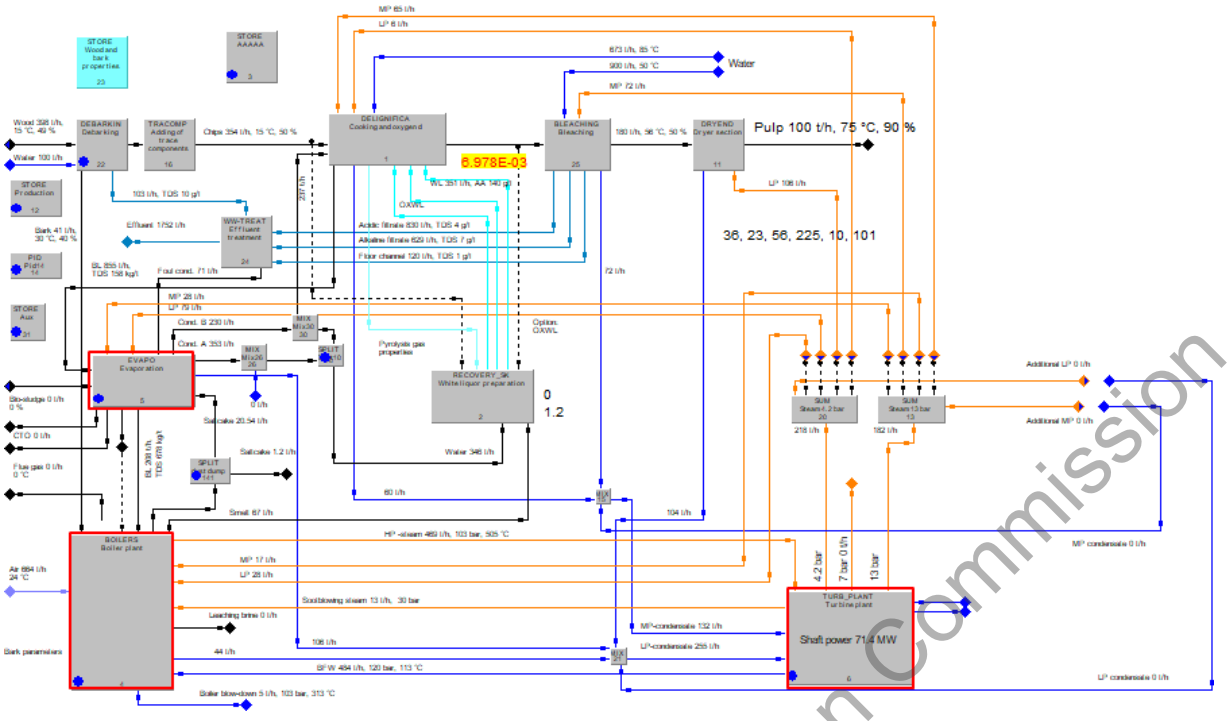

Figure 5. Overall flowsheet of the WinGEMS kraft pulp mill simulation model. The red rectangles indicate the simulation blocks with interfaces with the HTL-plant.

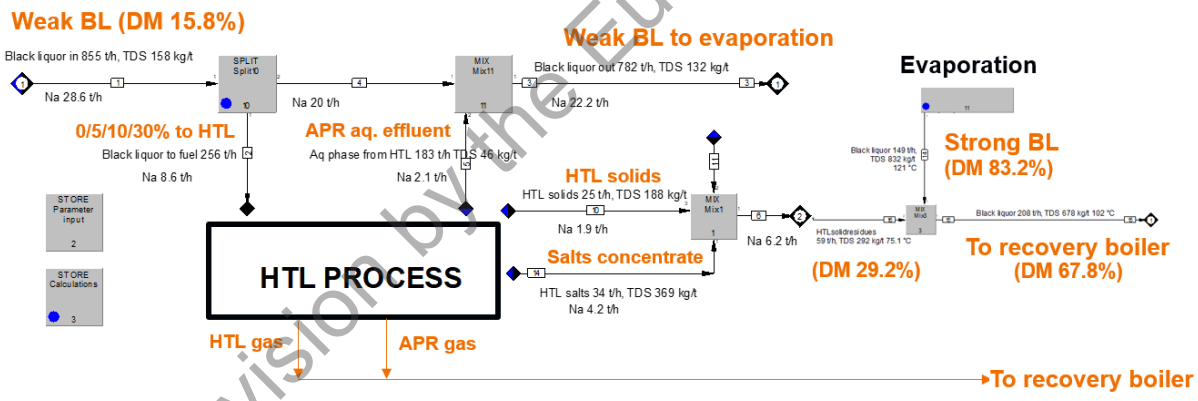

Figure 6. Print screen of the WinGEMS evaporation block with interfaces with the HTL plant.

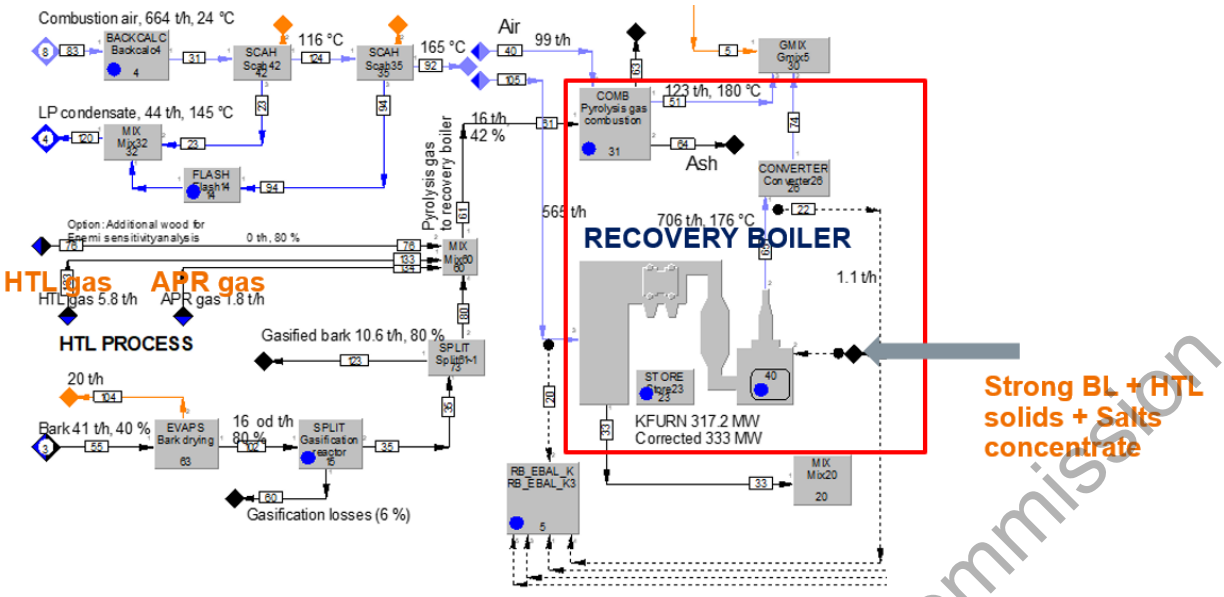

Figure 7 Print screen of the WinGEMS recovery boiler block with interfaces with the HTL plant.

4.1.4 Simulation of the BL2F-scenarios

Three BL2F-scenarios were simulated depending on the amount of black liquor sent to HTL plant. The total amount of weak black liquor in the reference scenario was 8.55 t/adt. Table 11 below presents the mass and energy flows (in t/adt) between the pulp mill and the HTL plant.

Table 11 Mass and energy flows (in t/adt) between the pulp mill and the HTL plant.

	From pulp mill to HTL			**From HTL to pulp mill**					
	BL to HTL	Steam		Salts	Solids	APR effluent	HTL gas	APR gas	Condensate
	t/adt	t/adt		t/adt	t/adt	t/adt	t/adt	t/adt	t/adt
BL2F5	0.43	0.02		0.06	0.04	0.31	0.01	0.003	0.02
BL2F10	0.86	0.03		0.11	0.08	0.61	0.02	0.01	0.03
BL2F30	2.57	0.10		0.34	0.25	1.83	0.06	0.02	0.10

The mass and energy balances of the BL2F-scenarios were stored in an Excel-spreadsheet for further analysis and comparison.

4.1.5 Comparison of the scenarios

The results expected from the integration modelling include lower recovery boiler thermal capacity due to lower amount and HHV of the black liquor feed to the boiler, lower electricity production due to lower boiler capacity, lower evaporation capacity due to lower black liquor amount to be evaporated and possible additional sodium or sulfur makeup requirements. The integration should not have any effects on cooking, O_2-delignification, bleaching or drying.

4.2 Results of the integration modelling

4.2.1 Boiler capacity and electricity production

Figure 21-Figure 24 in Annex C present the block diagrams with mass and energy balances for all four evaluated scenarios. The results are expressed as unit consumption per air dried tonne (adt) of pulp. In the block diagrams for BL2F-scenarios, the results are also compared with the Reference scenario. The difference (%) is presented in brackets.

Figure 8 shows how the integration of the HTL plant to pulp mill affects the pulp mill's recovery boiler thermal capacity (MW), total and net electricity productions (MW). In reference scenario, fuel feed to recovery boiler included pyrolysis gas from bark and strong black liquor (DM 83%). In BL2F-scenarios, the fuel feed included pyrolysis gas from bark, strong black liquor (DM 68%), HTL gas, APR gas, HTL solids and HTL salts.

In all evaluated scenarios, the pulp mill is self-sufficient regarding both heat and electricity. The recovery boiler thermal capacity decreases by 3, 6 or 17% when 5, 10 or 30% of black liquor is taken to HTL plant, respectively. The net electricity is surplus electricity that the pulp mill can sell out after meeting its own electricity consumption which is assumed to be 60 MW. The net electricity production decreases by 11, 23 or 69% when 5, 10 or 30% of black liquor is taken to HTL plant, respectively. There is still 11-33 MW electricity available for the HTL-plant.

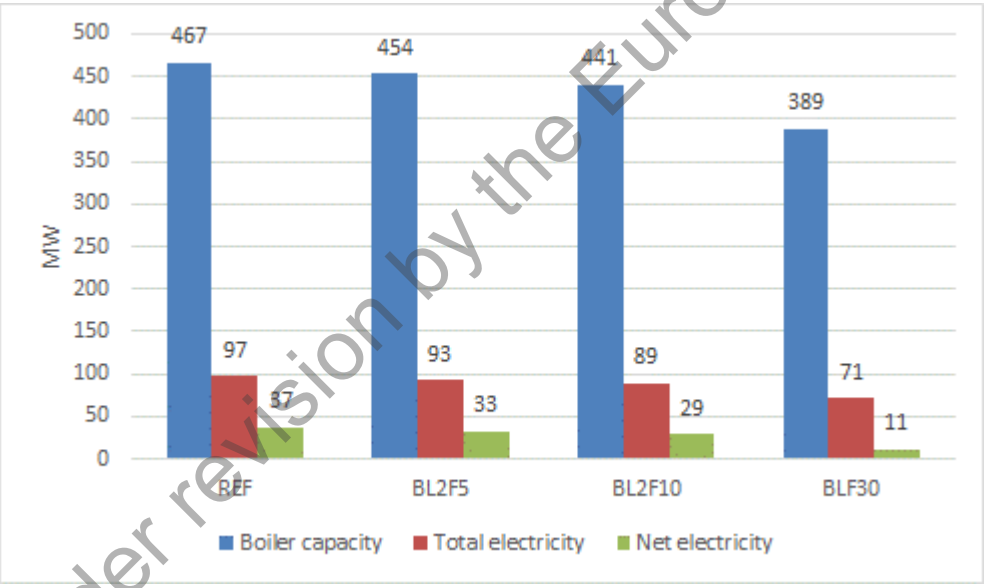

Figure 8 The effect of HTL-integration on the recovery boiler thermal capacity and total and net electricity productions of the pulp mill.

An interesting question is what would be the maximum amount of black liquor that could be treated in HTL plant without disturbing the self-sufficiency of the pulp mill. With the selected process design and assumptions, simulations indicate that 40% of black liquor can be directed to HTL plant with still having enough black liquor for producing enough heat and electricity for the pulp mill. In this BL2F40-scenarion, the boiler capacity decreases by 22% compared to reference scenario. The net electricity production would be 3 MW, thus 93 % lower than in the reference scenario.

4.2.2 Pulp mill's heat demand

Figure 9 shows how the integration of the HTL plant to pulp mill affects the pulp mill's heat demand (steam consumption) in different process departments. It has only effect on the heat demand of recovery boiler and evaporation. In recovery boiler, steam is used for heating the burning air. Due to the outtake of weak black liquor to HTL plant, the dry matter feed to recovery boiler decreases in BL2F-scenarios by 2-10%. It results that the heat demand needed to heat the burning air will decrease by 2-11%. The evaporation capacity (t water/t adt) decreases by 1%, 2% and 5% in BL2F5, BL2F10 and BLF30 scenarios. As a result, the heat demand in evaporation decreases by 1%, 2% and 5% compared to reference scenario.

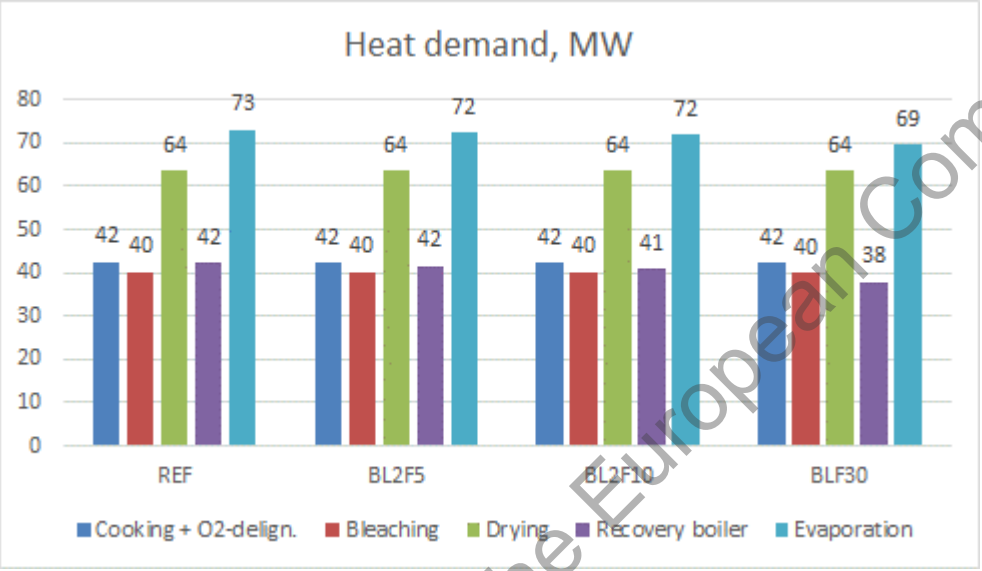

Figure 9 The heat demand (MW) in different process departments of the pulp mill. The integration of the HTL-plant does not affect cooking, O_2-delignification, bleaching or drying.

4.2.3 Pulp mill's sodium and sulfur balance

Table 12 presents how much sodium and sulfur is taken to the HTL plant via black liquor as well as recycled back via HTL side streams. The sulfur balance of the HTL plant indicates that sulfur should not be lost in HTL plant. Thus, the sulfur outtake from the pulp mill via weak black liquor equals almost the sulfur return via HTL streams. Instead, according to the balance calculation, a small addition of sulfur appears (0.3-0.5%). This is probably due to small decimal differences in the measured and modelled sulfur amounts of black liquor. Since the pulp mill and HTL plant modelling are iterative, small differences in the stream compositions occur.

The pulp mill's sodium balance, however, is affected by the integration. The sodium balance of the HTL plant indicates that some sodium is lost in HTL plant to crude oil. The sodium return via HTL streams is 3.1-3.3% less than the sodium outtake via weak black liquor. Thus, it is expected that there will be some additional sodium makeup need.

Table 12 Sodium and sulfur flows (kg/adt) between the pulp mill and HTL plant.

	From pulp mill to HTL		**From HTL to pulp mill**						**Loss/Gain in HTL**	
	BL		Salts		Solids		APR effluent			
	Na	S	Na	S	Na	S	Na	S	Na	S
	kg/adt	kg/adt	kg/adt	kg/adt	kg/adt	kg/adt	kg/adt	kg/adt	kg/adt	kg/adt
BL2F5	14.34	4.13	7.06	3.86	3.22	0.03	3.58	0.26	-0.47	0.01
BL2F10	28.67	8.26	14.13	7.72	6.45	0.06	7.16	0.51	-0.94	0.03
BL2F30	85.84	24.74	42.37	23.15	19.34	0.17	21.47	1.54	-2.65	0.12

Since neither of sodium nor sulfur amounts in the pulp mill are increased remarkably due to HTL integration, there is no need to increase the amount of dumped fly ash. Fly ash dumping from recovery boiler is needed to avoid the accumulation of potassium and chloride components. It may also be used to adjust the sodium and sulfur balances if sodium or sulfur start to accumulate for some reason to pulp mill's chemical cycle. Figure **10** shows the amounts of sodium and sulfur that are dumped along the fly ash. Their amounts are almost the same in all evaluated scenarios, since the amount of dumped fly ash was kept constant (12 kg/adt).

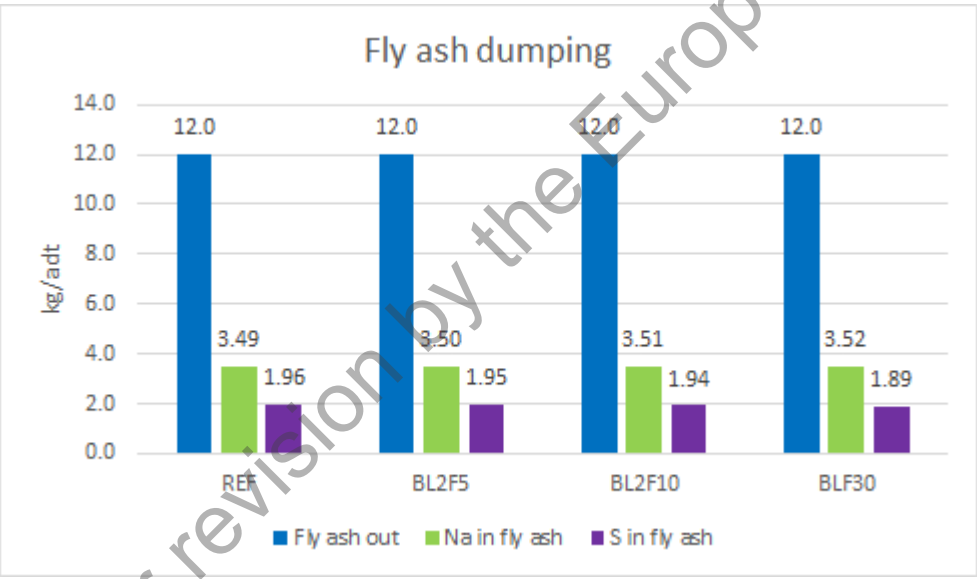

Figure 10 Amount of dumped fly ash (kg/adt) and sodium and sulfur losses (kg/adt) along the fly ash for all evaluated scenarios

Figure 11 presents how the integration of the HTL plant affects the makeup amounts of cooking chemicals (NaOH and Na_2SO_4) and the amounts of sodium and sulfur that come in along with the cooking chemicals. Sodium makeup need increases by 7%, 15% and 44% in BL2F5, BL2F10 and BL2F30 scenarios, respectively. The increases in absolute values, 0.5, 0.9 and 2.7 kg/adt equal the lost in HTL plant presented in Table 12. The small decrease in the makeup need of sulfur (0.04-0.2 kg/adt) derives from the small balance error explained above. In true process, small amounts of sulfur will end up in the crude oil, and thus HTL integration will increase a little the sulfur intake to pulp mill.

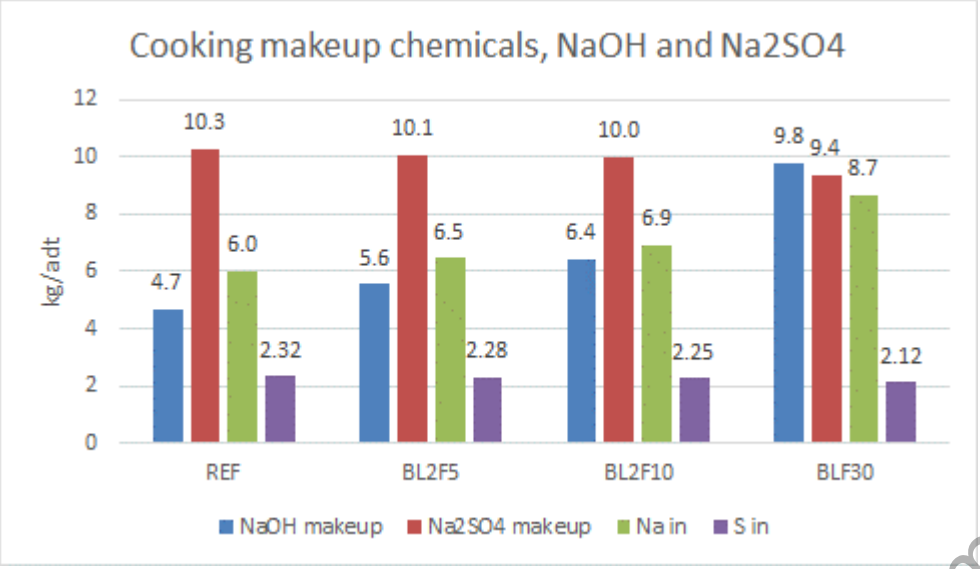

Figure 11. The effect of HTL integration on pulp mill's cooking chemical makeup amounts

Figure 25 in Annex D show the total sodium and sulfur balance across the pulp mill. The main source for sodium and sulfur input in the reference scenario is bleaching chemicals constituting of 66% of sodium input and 53% of sulfur input. In BL2F-scenarios, most of the sodium (44-80%) and sulfur (42-81%) come in among the HTL recycle streams. The main source for sodium and sulfur output in the reference scenario is wastewater constituting of 76% of sodium output and 65% of sulfur output. In BL2F-scenarios, most of the sodium (45-83%) and sulfur (42-81%) leaves the pulp mill via weak black liquor feed to HTL-plant.

4.2.4 Pulp mill's water balances

The integration of the HTL plant has negligible effect on pulp mill's freshwater consumption. In BL2F-scenarios, the freshwater consumption increases by 0.3-1.8 % compared to the reference scenario. The integration of HTL plant has no effect on the wastewater amount. The cooling water consumption in turbine plant decreases by 10-60 % and in evaporation by 1-7 % compared to reference scenario.

5 Analysis of the upgrading of the HTL oil at refinery

5.1 Modelling

5.1.1 Approach

The process model is developed in Aspen HYSYS V12.1. The taken approach represents the material streams through modelling components and significantly reduces the complexity of the real process. The overall flow sheet of the upgrading process is shown in Figure 12. Five main processes can be distinguished: Hydrotreater, Separation, Fractionation, Hydrocracking and the H_2 recycling/ Gas treatment. In this preliminary result, the hydro-isomerization of the naphtha fraction, to increase the kerosene and diesel yield, is not included. The selected fluid package was UNIQUAQ (Bouillot et al., 2022).

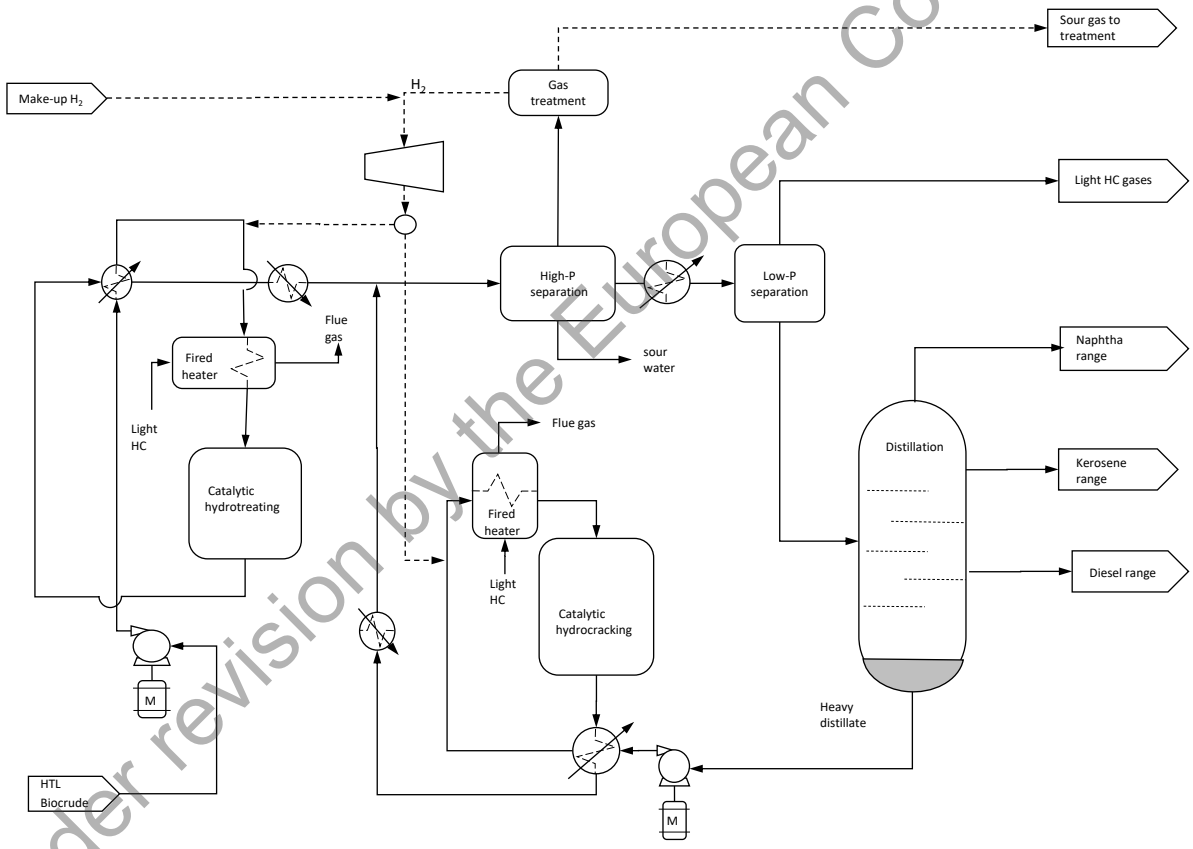

Figure 12: Overall process flow sheet of the biocrude upgrading

5.1.2 HTL oil model

A mixture of 40 components, corresponding to typical components formed during the HTL of lignin, cellulose and hemicellulose based feedstocks as well as common hydrotreated products of those components (do Couto Fraga et al., 2021; Malins, 2017; Mathanker et al., 2020; Gollakota et al., 2018; Pedersen et al., 2017) were selected to represent the oil from the HTL

plant. The salt content is simplified and represented by NaOH. The complete list of components is shown in Annex B. To determine the concentration of the respective components, a multi-objective optimization was implemented (Lozano et al., 2019). The objective functions correspond to the differences between the oil properties which were calculated in the HTL process modelling analysis (see Section 3) and the oil properties based on the model component mixture

$$\frac{\left(HHV_{exp} - \sum_{i=1}^{n} X_i HHV_i\right)}{HHV_{exp}} = F_1,$$

$$\frac{\left(C_{exp} - \sum_{i=1}^{n} X_i C_i\right)}{C_{exp}} = F_2,$$

$$\frac{\left(H_{exp} - \sum_{i=1}^{n} X_i H_i\right)}{H_{exp}} = F_3,$$

$$\frac{\left(O_{exp} - \sum_{i=1}^{n} X_i O_i\right)}{O_{exp}} = F_4,$$

$$\frac{\left(S_{exp} - \sum_{i=1}^{n} X_i S_i\right)}{S_{exp}} = F_5,$$

where C, H, O and S correspond to elemental composition in wt% and X_i to the mass fraction of the component i. Several constraints were given to limit the number of possible solutions, i.e. $\sum_{i=0}^{n} X_i = 1$ and the distribution was constrained loosely to yield values (in terms of the boiling point distributions) similar to the ones observed in literature for hydrotreated HTL oils (Pedersen et al., 2017). The overall objective was then to minimize the sum of the objective functions $F_i(x)$. Table 13 shows the elemental analysis and higher heating value of the model oil. The resulting component concentrations of the optimization procedure can be found in the Annex E.

Table 13: Results of the biocrude optimization

	Results from HTL modelling	Model oil
C (dry wt%)	85.1718	83.9643
H (dry wt%)	8.0346	10.416
O (dry wt%)	3.8391	3.8391
N (dry wt%)	0	0
S (dry wt%)	0.0014	0.0018
HHV [MJ/kg]	37.6	39.8

5.1.3 Hydrotreater

The biocrude entering the upgrading went already through a hydrotreating stage downstream of the HTL plant (see Sect 4.) and has a low metal and sulphur content. Therefore, the inclusion of a guard reactor, to restrict catalyst poisoning, is deemed unnecessary. The biocrude, is heated up (through a heat exchanger with the effluents of the hydrotreater and a fired heater, to 360°C), pressurized (100bar) and mixed with hydrogen in a 1/5 mol Oil/mol H_2 ratio (Hoekstra, 2007). The overall process in the hydrotreating reactor is modelled by a conversion

reactor with simplified hydrotreating reactions for the components that include oxygen/sulphur and selected decarboxylation reactions. The overall conversion is assumed to be 80% based on the expected deoxygenation from literature (Jarvis et al., 2018). The considered reactions are:

$$C_4H_{10}O_2 + 2H_2 \rightarrow C_4H_{10} + H_2O$$
$$C_7H_8O_2 + 2H_2 \rightarrow C_7H_8 + 2H_2O$$
$$C_6H_6O + H_2 \rightarrow C_6H_6 + H_2O$$
$$C_7H_8O + H_2 \rightarrow C_7H_8 + H_2O$$
$$C_8H_{10}O + H_2 \rightarrow C_8H_{10} + H_2O$$
$$C_5H_8O_3 + 3H_2 \rightarrow C_5H_8 + 3H_2O$$
$$C_{10}H_{20}O_4 + 5H_2 \rightarrow C_{10}H_{22} + 4H_2O$$
$$C_5H_4O_2 + 4H_2 \rightarrow C_5H_8 + 2H_2O$$
$$C_{16}H_{32}O_2 \rightarrow C_{15}H_{32} + CO_2$$
$$C_{16}H_{32}O_2 + 2H_2 \rightarrow C_{16}H_{32} + 2H_2O$$
$$C_3H_4O_2 + 2H_2 \rightarrow C_3H_4 + 2H_2O$$
$$C_2H_4O_2 \rightarrow CH_4 + CO_2$$
$$C_2H_4O_2 + 2H_2 \rightarrow C_2H_4 + 2H_2O$$
$$CH_4O + H_2 \rightarrow CH_4 + H_2O$$
$$C_{18}H_{36}O_2 + 3H_2 \rightarrow C_{18}H_{38} + 2H_2O$$
$$C_{18}H_{34}O_2 + 4H_2 \rightarrow C_{18}H_{38} + 2H_2O$$
$$C_{18}H_{34}O_2 \rightarrow C_{17}H_{34} + CO_2$$
$$C_{20}H_{40}O_2 \rightarrow C_{19}H_{40} + CO_2$$
$$C_{18}H_{36}O_2 \rightarrow C_{17}H_{36} + CO_2$$
$$C_{12}H_8S + H_2 \rightarrow C_{12}H_8 + H_2S$$

5.1.4 Separation and fractionation

The biocrude from the HTL plant has a relatively high salt content, which must be removed in an upgrading stage. Modern Desalting processes usually employ an electrostatic desalter, which cannot be modelled in HYSYS. As a simplification, the desalter is represented by a component splitter removing the salt in the separation stage. Further, the separation stage includes a high-pressure, low temperature three phase separator (p=100bar, T=40°C). The gaseous fraction is led to the gas treatment while the liquid fraction is fed into the atmospheric distillation column that separates lights, water, naphtha, kerosene, diesel, and the heavy fraction which is processed in the hydrocracker.

5.1.5 Hydrocracker

The hydrocracking is performed at high pressure and temperature (p=100bar, T=360°C). Like the hydrotreating stage, the hydrocracking is modelled by a conversion reactor with simplified reactions for the heavy fraction of the oil:

$$C_{16}H_{32}O_2 + 2H_2 \rightarrow C_{16}H_{32} + 2H_2O$$
$$C_{18}H_{36}O_2 + 3H_2 \rightarrow C_{18}H_{38} + 2H_2O$$
$$C_{18}H_{34}O_2 + 4H_2 \rightarrow C_{18}H_{38} + 3H_2O$$
$$C_{18}H_{38} + H_2 \rightarrow C_{11}H_{24} + C_7H_{16}$$
$$C_{14}H_{10} + 3H_2 \rightarrow C_8H_{10} + C_6H_6$$

5.1.6 Gas treatment

The gas treatment is modelled with the acid gas chemical solvents property package from HYSYS which was developed to model the removal of acids gases such as H_2S and CO_2. Methyl diethanolamine (MDEA) is used as the solvent. The reactions and chemistry for this case are automatically generated by Aspen HYSYS using the underlying thermodynamics and calculation models that are included in the property package (AspenTech, 2017). The corresponding flow sheet is shown in Figure 13 and includes an absorber column, a separator, the regenerator distillation column, and the blending of the make-up H_2 into the treated sweet gas stream. The process is modelled separately from the main process, delimited by stream cutters that calculate the transition between the two property packages and component lists. The reason for this is that the acid gas chemical solvents property package does not include the thermodynamical properties for some of the spurious heavier components that are send to the gas cleaning, which restricts the convergence of the absorber and regenerator columns. The transfer basis of the stream cutters is set to T-P flash and the component list is reduced to 20 components (the heavier components are discarded). The resulting mass imbalance for the stream cutters is below 0.1%.

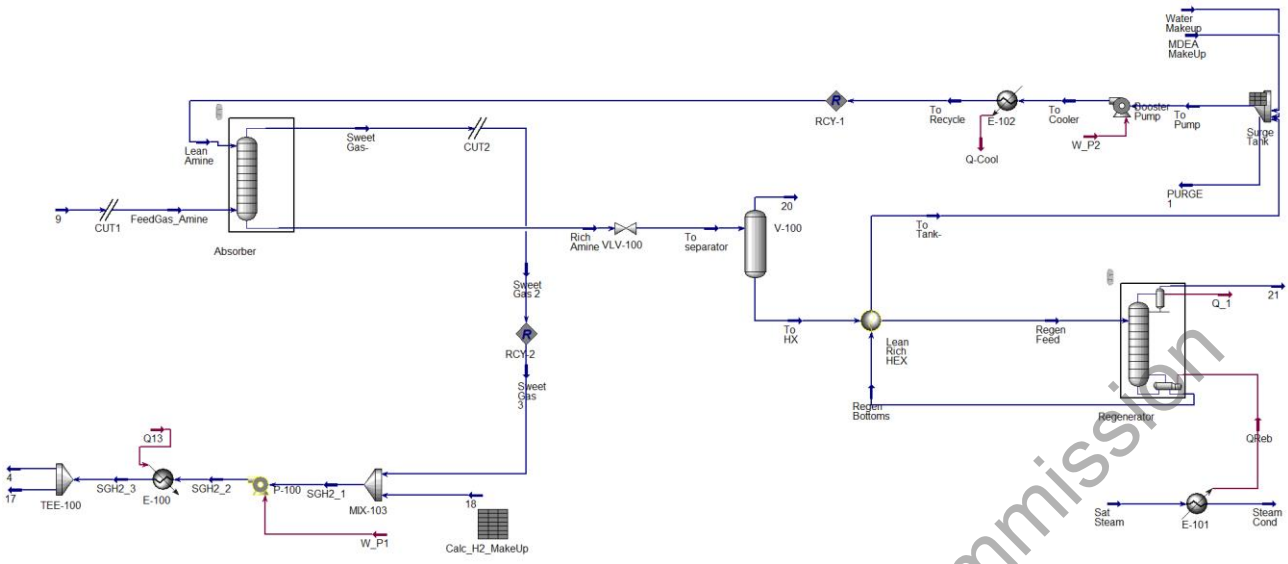

Figure 13: Flow sheet Gas Treatment

5.2 Results

Figure 26 and Table 16 in Appendix E shows the calculated flows of the HTL biocrude upgrading process. Table 14 specifies the main product fractions considered in the analysis and their respective calculated yields. The major fraction of the upgraded oil lies in the naphtha range. To increase the share of aviation and marine fuels (i.e., kerosene and diesel range), the naphtha must undergo an isomerization process, which for these preliminary results is not considered in the process analysis. Table 13 shows the calculated mass flow rates for the main streams in the upgrading process scheme considered for the upgrading of HTL biocrude derived from black liquor to naphtha, kerosene and diesel.

Table 14: Temperature range of the products and predicted yields of the upgrading process

Stream number	12	14	15	16
Fraction	Light hydrocarbons	Naphtha	Kerosene	Diesel
TBP [°C]	< 80	80-180	180-220	220-300
Carbon [%wt]	84.1	88.7	86.2	86.4
Hydrogen [%wt]	12	10.9	12.1	13
HHV [MJ/kg]	44.4	44.2	44.3	45.3
Mass yield (dry basis)	0.071	0.242	0.201	0.343
Energy yield (based on HHV)	0.08	0.27	0.22	0.39

Table 15: Main mass flows calculated for the upgrading of the HTL biocrude derived from black liquor to naphtha, kerosene and diesel.

Biocrude feed	kg/h	3600
Organic liquid to distillation	kg/h	4845
Light HC from distillation	kg/h	255
Naphtha range from distillation	kg/h	871
Kerosene range from distillation	kg/h	725
Diesel range from distillation	kg/h	1235
Heavy fraction from distillation	kg/h	1695
Process water	kg/h	244
Sour gas from separation	kg/h	29
Total make-up H_2	kg/h	47.5
Consumption in hydrotreating	kg/h	36.6
Consumption in hydrocracking	kg/h	10.9
Fuel gas consumption	kg/h	32.64
Make-up amine consumption	kg/h	1.01

6 Conclusions and future work

6.1 HTL plant and biocrude upgrading

The process design for the conversion of black liquor to biofuels has been described through detailed process flow diagrams. The overall conversion process includes a decentralized HTL plant integrated into the pulp mill, where the black liquor is converted by hydrothermal liquefaction to an oil-phase product or biocrude, and further upgrading of the HTL biocrude in a refinery. The main challenges in the HTL conversion are: 1) the high salts content in the black liquor, which can cause severe fouling and corrosion in the HTL reactor, and 2) the high oxygen and sulphur content in the oil product after the HTL process, which can be above the limits that can be accepted by conventional refineries. To solve these challenges, the design the HTL plant process includes: 1) initial salts precipitation integrated in the same HTL reactor, 2) partial catalytic hydrotreating of the HTL product to remove oxygen and sulphur heteroatoms. The hydrogen required for this hydrotreating process is produced at the HTL plant by aqueous phase reforming of the liquid effluent separated after hydrotreating. The overall conversion of black liquor to biocrude has been estimated to have a dry mass and chemical energy yield of approximately 16% and 42% respectively. The process design for the upgrading of the HTL oil to biofuels at refinery considers first a second catalytic hydrotreating to fully remove oxygen and sulphur from the oil feed, followed by fractionation to naphtha, kerosene, diesel, and heavy distillate. The heavy distillate can be further converted by hydrocracking to more naphtha, kerosene, and diesel. Naphtha can be further converted to aviation fuel by hydro-isomerization. The yields for naphtha, kerosene and diesel relative to the biocrude feed into the upgrading are 24.2%, 20.1% and 34.3% on dry mass basis and 27%, 22% and 39% on chemical energy basis, respectively. Since most of the relevant experimental results are still not available, the flow calculations for the HTL plant and the biocrude upgraded process included in this deliverable are preliminary and based on estimated values for the transfer coefficients defined in the empirical models described in Sections 3 and 5. An update of the flow calculations using the whole set of experimental results from the project will be reported as part of the scale-up analysis in deliverable D4.2.

6.2 Integration of the HTL plant into the pulp mill

The effects of the integration of a HTL plant to a hardwood kraft pulp mill was studied using process simulation. An existing plant wide process simulation model was used for calculating the mass and energy balances for the reference scenario, i.e., a hardwood kraft pulp mill. The HTL integration was conducted by taking part of the weak black liquor from pulp mill and treating it in the HTL plant for producing crude bio-oil. The side streams of the HTL plant (solids, aqueous and gas streams) were recycled back to the pulp mill for recovering cooking chemicals (sodium and sulfur) and heat content.

The compositions of the HTL side streams recycled back to pulp mill derived from HTL plant modelling. Required modifications were done for the reference scenario model to study the effects of the HTL integration. Three BL2F-scenarios were simulated with varying the amount of black liquor (5%, 10% and 30%) sent to HTL plant. The simulation model considered the changes in the dry matter content and heating value in the feeds to evaporation and recovery boiler due to the integration of the HTL plant.

Preliminary results for the integration of the HTL plant to hardwood pulp show that if 30% of weak black liquor is directed to HTL, compared to the reference scenario:

- recovery boiler capacity decreases by 17%
- net electricity production decreases by 69%
- heat demand in boiler plant decreases by 11%
- evaporation heat demand decreases by 5%
- sodium intake via cooking chemicals (NaOH, Na_2SO_4) increases by 45%
- sulfur intake via cooking chemicals (Na_2SO_4) decreases by 9%
    - (The decrease is probably due to small balance error in modelling.)
- cooling water consumption in turbine plant decreases by 60%
- cooling water consumption in evaporation decreases by 7%

The integration of the HTL plant to pulp mill has no effect on the amount of dumped fly ash or delignification and bleaching chemicals. It has only negligible effects on freshwater consumption or wastewater production.

An interesting question is what would be the maximum amount of black liquor that could be treated in HTL plant without disturbing the self-sufficiency of the pulp mill. With the selected process design and assumptions, simulations indicate that 40% of black liquor can be directed to HTL plant with still having enough black liquor for producing enough heat and electricity for the pulp mill. In this BL2F40-scenarion, the boiler capacity decreases by 22% compared to reference scenario. The net electricity production would be 3 MW, thus 93 % lower than in the reference scenario.

To enhance the electricity production additional feedstock to the HTL process or the recovery boiler could be considered. The extra feedstock to the HTL process would decrease the BL usage and the leave more BL for the combustion at the recovery boiler. Support fuel at the recovery boiler would produce more electricity and compensate the reduced electricity production. Naturally, if applicable the pulping capacity of the mill might be increased in order to run the recovery boiler at full capacity. All the cases require further investigations.

The presented results are preliminary and based on computational compositions of the HTL streams. After the pilot HTL reactor operates properly and produces concrete product streams, the integration modelling studies can be updated with measured stream compositions.

7 Bibliography

AspenTech. (2017). Jump Start Acid Gas Cleaning in Aspen HYSYS V10.

Bouillot, B. (2022). Introduction to Thermodynamic Methods for Process Engineering, Choice of a thermodynamic model and simulation.

Gollakota, A.R.K., Kishore, N., Gu, S. (2018). A review on hydrothermal liquefaction of biomass. Renewable and Sustainable Energy Reviews, 81 (1), 1378-1392.

Hoekstra, G. (2007). The effects of gas-to-oil rate in ultra low sulfur diesel hydrotreating. Catalysis today, 127 (1-4), 99-102.

Jarvis, J.M., Albrecht, K.O., Billing, J.M., Schmidt, A.J., Hallen, R.T., Schaub, T.M. (2018). Assessment of Hydrotreatment for Hydrothermal Liquefaction Biocrudes from Sewage Sludge, Microalgae, and Pine Feedstocks. Energy&Fuels, 32 (8), 8483-8493.

Kangas, P., Kaijaluoto, S., Määttänen, M. (2014). Evaluation of future pulp mill concepts – Reference model of a modern Nordic kraft pulp mill. Nord. Pulp Pap. Res. J. 29 (4), 620-634.

Lozano, E.M., Pedersen, T.H., Rosendahl, L.A. (2019). Modeling of thermochemically liquefied biomass products and heat of formation for process energy assessment. Applied Energy, 254 (15), 113654.

Malins, K. (2017). Production of bio-oil via hydrothermal liquefaction of birch sawdust. Energy Conversion and Management, 144 (15), 243-251.

Mathanker, A., Pudasainee, D., Kumar, A., Gupta, R. (2020). Hydrothermal liquefaction of lignocellulosic biomass feedstock to produce biofuels: Parametric study and products characterization. Fuel, 271, 117534.

Pedersen, T.H., Jensen, C.U., Sandström, L, Rosendahl, L.A. (2017). Full characterization of compounds obtained from fractional distillation and upgrading of a HTL biocrude. Applied Energy, 202, 408-419.

Annex A. Process Flow Diagrams

This section contains the detailed process flow diagrams for the main systems included in the HTL oil production plant and the upgrading of the HTL oil to marine and aviation fuels.

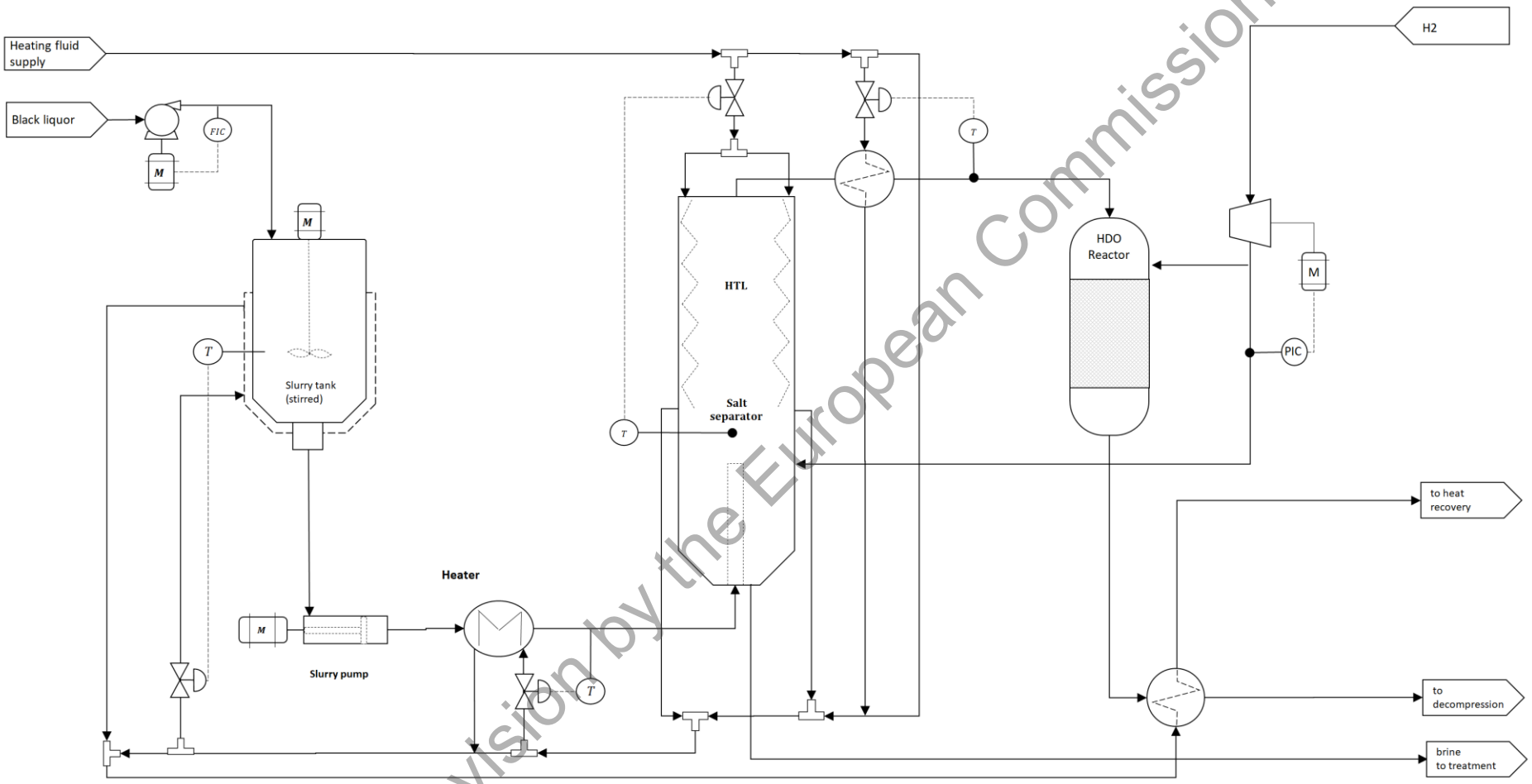

Figure 14: Process flow diagram for the black liquor feeding, pressurization, heating, integrated salt separation and liquefaction, and first-stage hydrodeoxygenation.

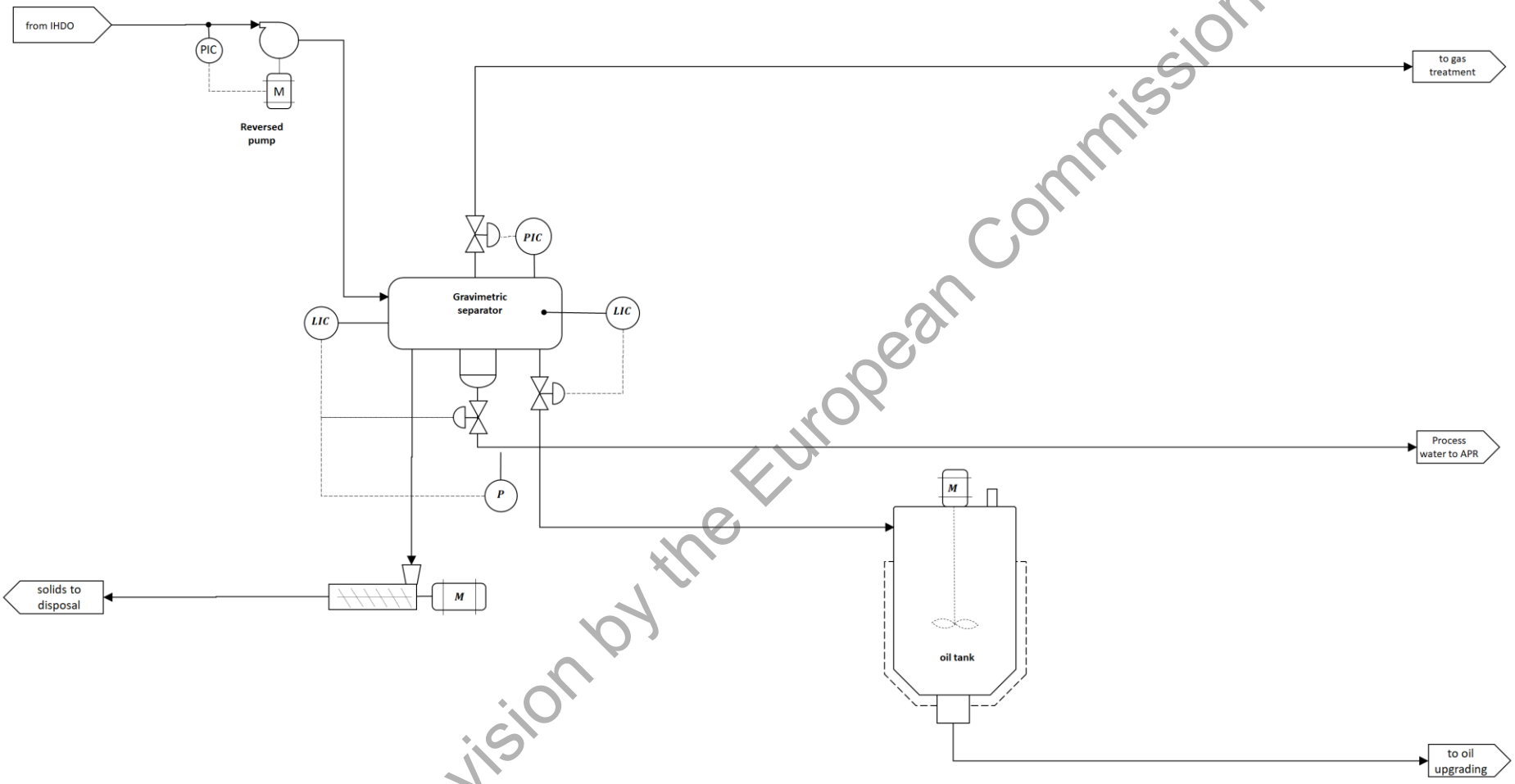

Figure 15: Process flow diagram for the separation of gas, oil, aqueous and solid phases of the product after the first-stage hydrodeoxygenation (HDO-I).

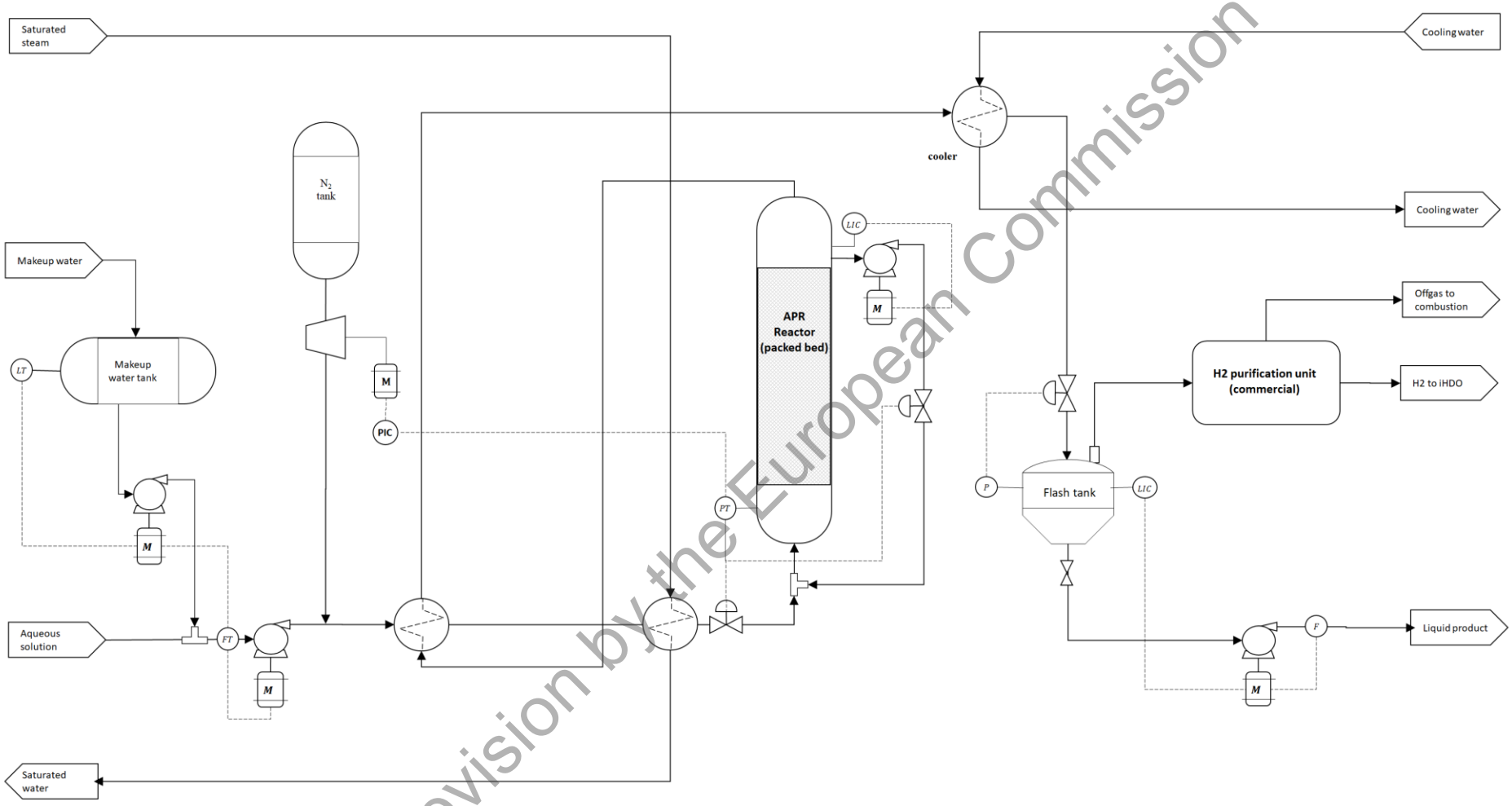

Figure 16: Process flow diagram for the aqueous phase reforming (APR) of the aqueous effluent after HDO-I.

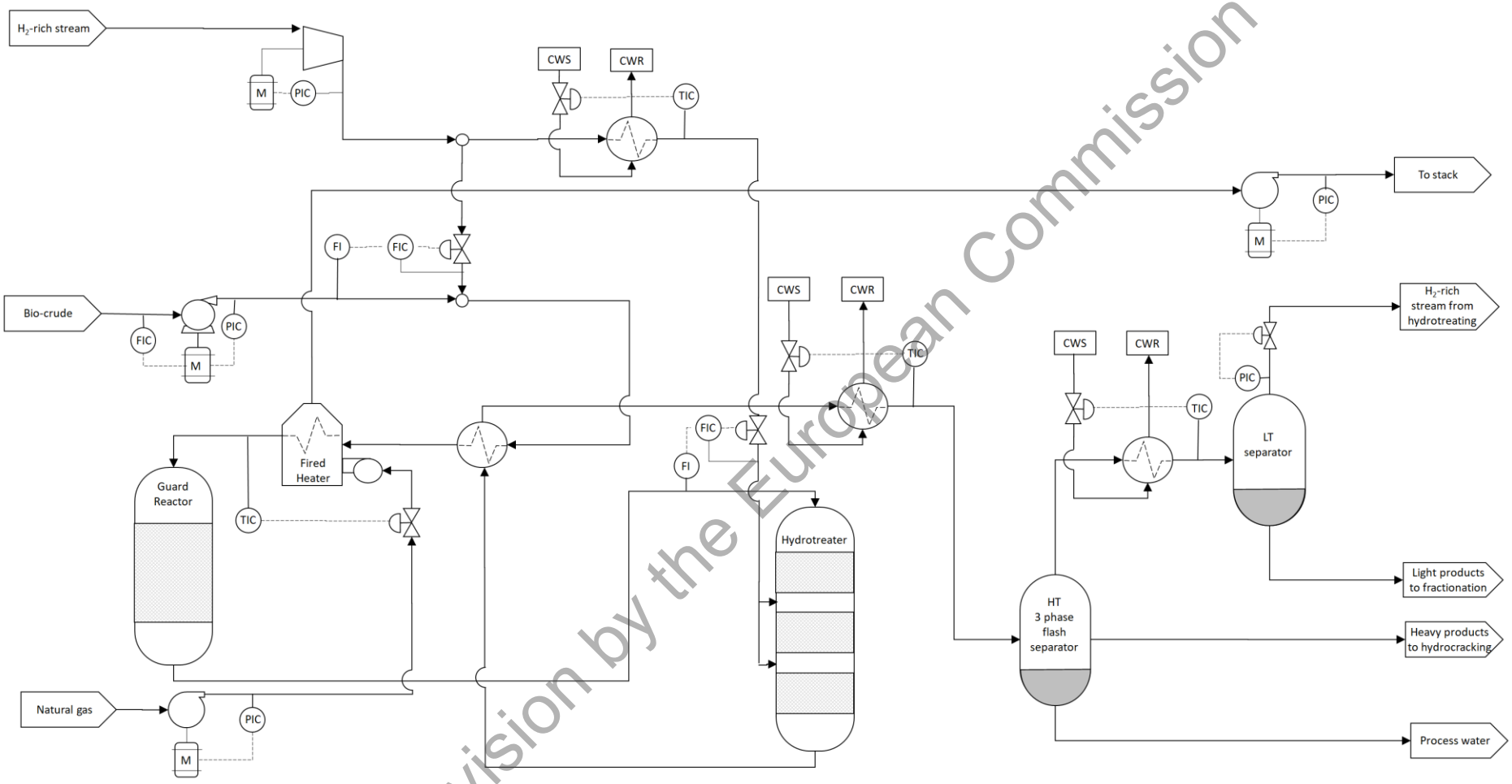

Figure 17: Process flow diagram for the inorganics separation and hydrotreating of black liquor derived HTL-oil followed by two-stage separation of the gas, process water and organic liquid phases.

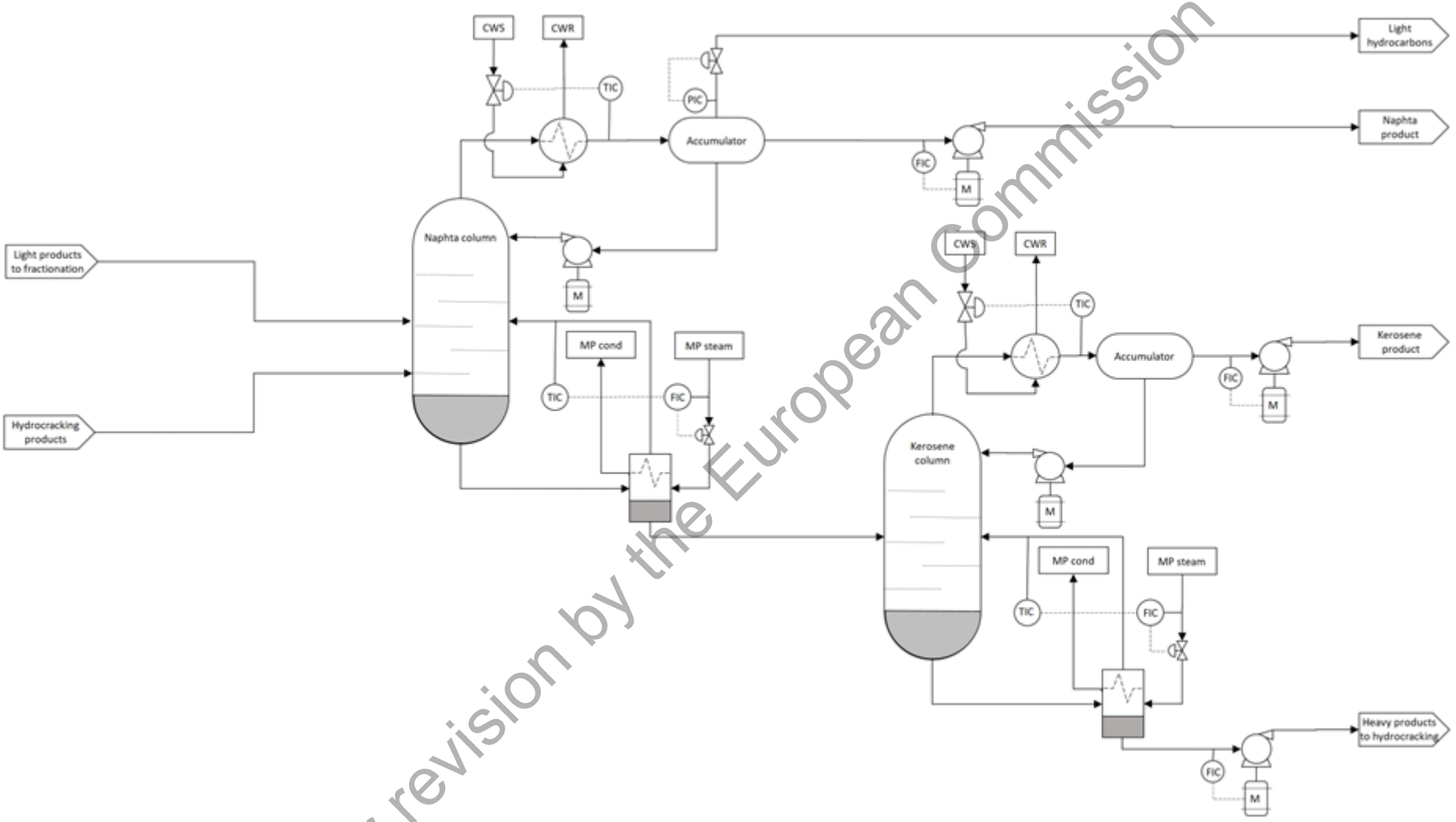

Figure 18: Process flow diagram for the fractionation of the organic liquid from hydrotreating to naphtha and kerosene by distillation.

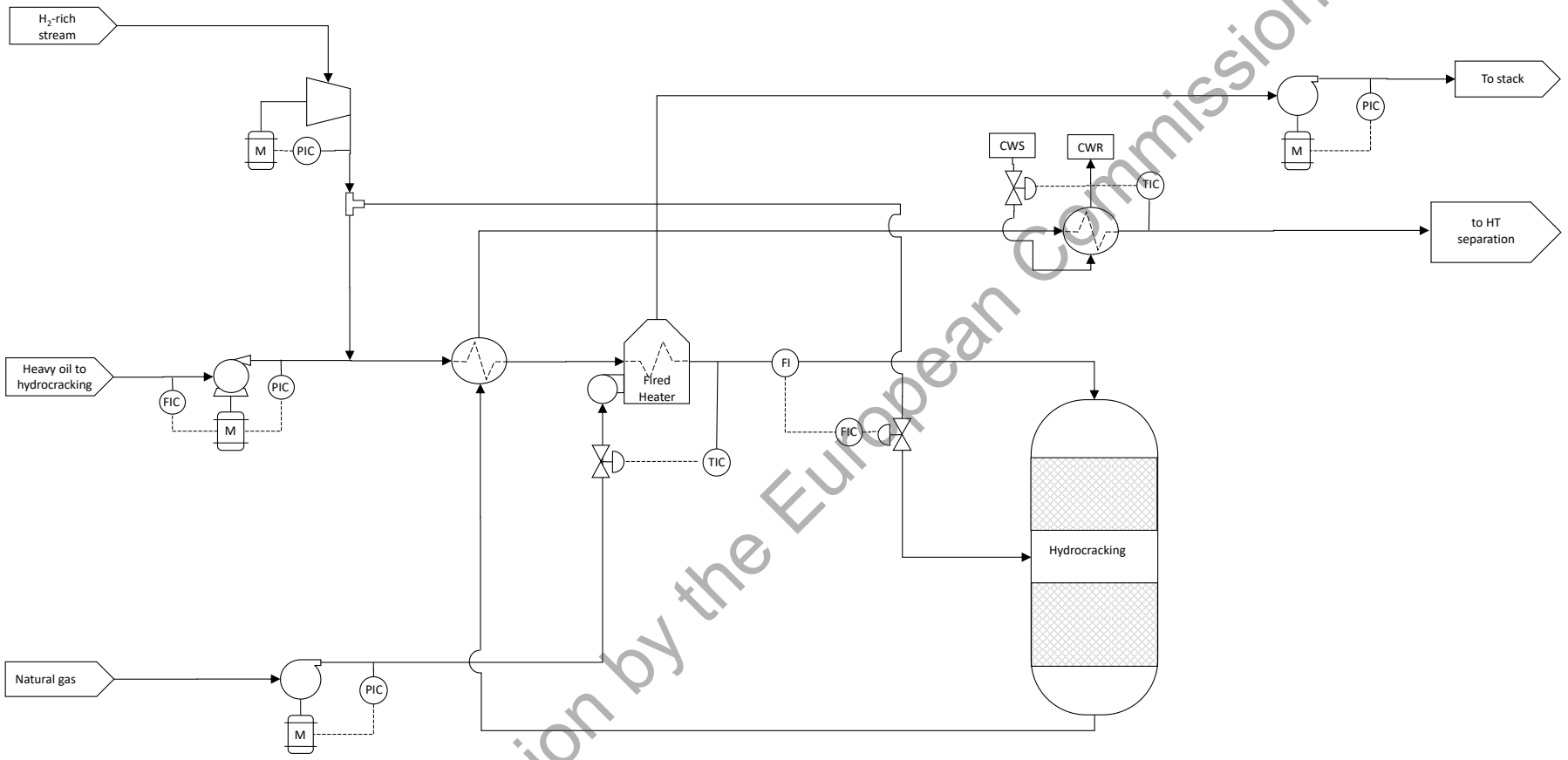

Figure 19: Process flow diagram for the hydrocracking of heavy fraction from the kerosene distillation column

Annex B. Mass and energy flows for the HTL plant

This section contains preliminary estimations of the material and energy flows associated to the HTL plant

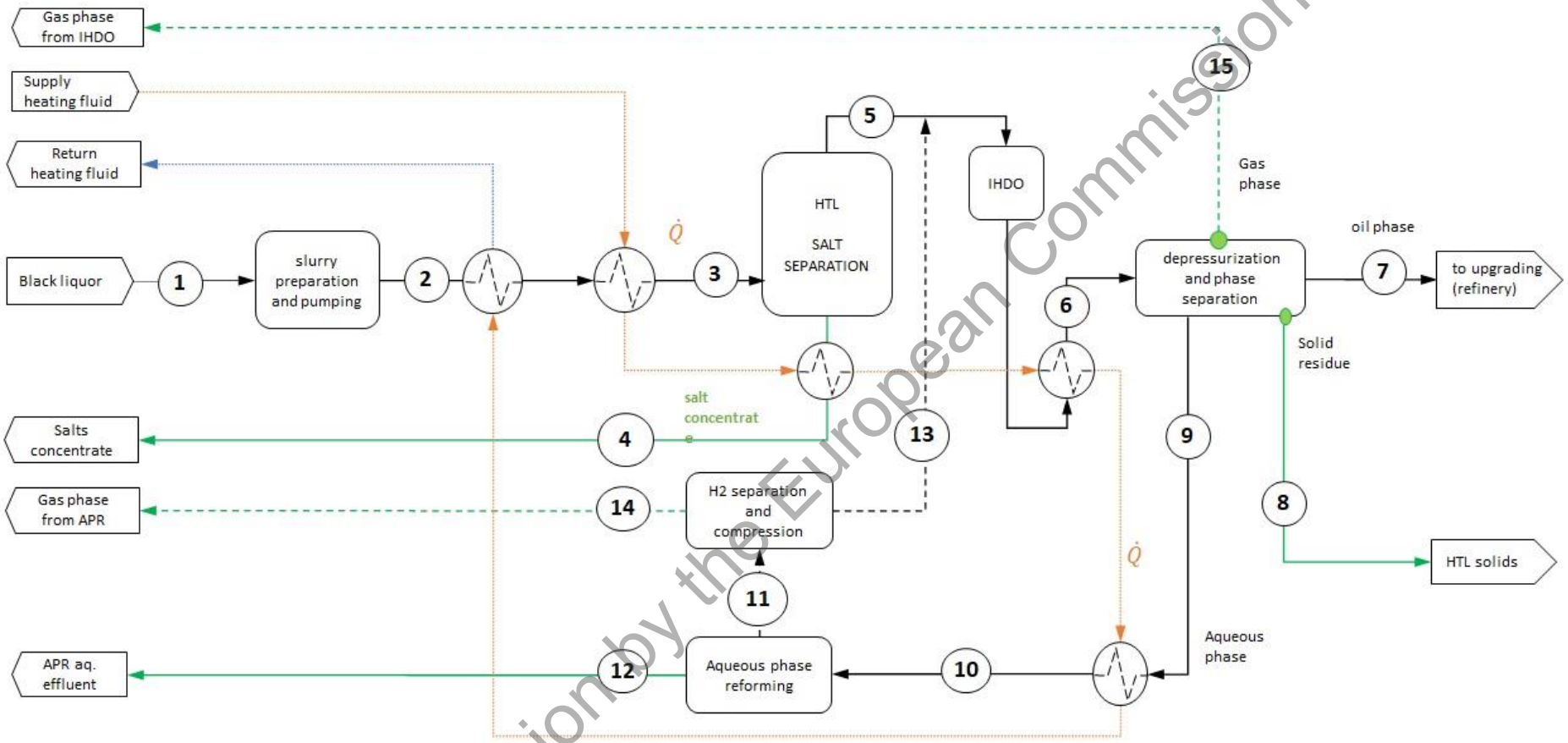

Figure 20: Process block diagram of the HTL plant process with numbering of the flows included in the calculations

Table 16: Preliminary calculations of the material and energy flows for the HTL plant

Flow no.	1	2	3	4	5	6	7
Fluid	Raw feedstock	Pressurized slurry	Preheated slurry	Cooled salt concentrate	HTL product	IHDO product cooled	HTL Oil product
Temperature (°C)	101,00	122,60	350,00	105,00	350,00	150,00	40,00
Pressure (bar-g)	1,01	320,00	320,00	2,00	320,00	30,00	1,01
Normal Flow Rate (Nm3/h)							
Mass Flow Rate (kg/s)	0,476	0,476	0,476	0,064	0,412	0,413	0,012
HHV (MJ/kg dry)	13,30	13,30	13,30	4,26	17,40	18,75	35,68
Chemical enthalpy (MW)	1,000	1,000	1,000	0,100	0,900	0,983	0,424
Thermal enthalpy (MW)	0,153	0,173	0,847	0,016	0,847	0,204	0,000
Total enthalpy (MW)	1,153	1,173	1,847	0,116	1,747	1,187	0,427
ATOMIC COMPOSITION							
Water (%wt)	84,20	84,20	84,20	63,06	87,46	87,31	1,49
Dry Matter (%wt)	15,80	15,80	15,80	36,94	12,54	12,69	98,51
Carbon, C (%wt dry)	33,89	33,89	33,89	12,66	43,52	42,97	85,17
Hydrogen, H (%wt dry)	4,13	4,13	4,13	2,20	5,01	6,24	8,03
Oxygen, O (%wt dry)	31,07	31,07	31,07	27,37	32,75	32,31	3,84
Nitrogen, N (%wt dry)	0,00	0,00	0,00	0,00	0,00	0,00	0,00
Sulfur, S (%wt dry)	6,13	6,13	6,13	18,29	0,61	0,61	0,00
Phosphorous, P (g/kg dry)	0,05	0,05	0,05	0,02	0,07	0,07	0,00
Calcium, Ca (g/kg dry)	0,00	0,00	0,00	0,00	0,00	0,00	0,00
Aluminium, Al (g/kg dry)	0,01	0,01	0,01	0,00	0,01	0,01	0,00
Iron, Fe (g/kg dry)	0,00	0,00	0,00	0,00	0,00	0,00	0,00
Magnesium, Mg (g/kg dry)	0,30	0,30	0,30	0,10	0,40	0,39	0,00
Potassium, K (g/kg dry)	37,29	37,29	37,29	59,52	27,20	26,84	2,41
Chlorine, Cl (g/kg dry)	0,48	0,48	0,48	0,15	0,63	0,62	0,00
Sodium, Na (g/kg dry)	209,57	209,57	209,57	335,03	152,63	150,61	27,10
Silicon, Si (g/kg dry)	0,02	0,02	0,02	0,01	0,03	0,03	0,01
Manganese, Mn (mg/kg dry)	90,55	90,55	90,55	29,01	118,48	0,00	0,01
SALTS COMPOSITION							
NaOH (kg / kg dry)	5,91E-02	5,91E-02	5,91E-02	0,00E+00	0,00E+00	0,00E+00	0,00E+00
Na2S (kg / kg dry)	0,00E+00	0,00E+00	0,00E+00	0,00E+00	0,00E+00	0,00E+00	0,00E+00
NaHS (kg / kg dry)	9,44E-02	9,44E-02	9,44E-02	0,00E+00	0,00E+00	8,53E-03	1,88E-05
Na_2SO_4 (kg / kg dry)	2,75E-02	2,75E-02	2,75E-02	0,00E+00	0,00E+00	3,91E-03	8,61E-06
Na_2SO_3 (kg / kg dry)	0,00E+00	0,00E+00	0,00E+00	0,00E+00	0,00E+00	0,00E+00	0,00E+00
$Na_2S_2O_3$ (kg / kg dry)	2,86E-03	2,86E-03	2,86E-03	0,00E+00	0,00E+00	7,38E-04	1,63E-06
Na_2CO_3 (kg / kg dry)	3,36E-02	3,35E-02	3,35E-02	0,00E+00	0,00E+00	8,22E-04	1,81E-06
K_2CO_3 (kg / kg dry)	2,92E-02	2,92E-02	2,92E-02	0,00E+00	0,00E+00	0,00E+00	0,00E+00

Table 17(cont.): Preliminary calculations of the material and energy flows for the HTL plant

Flow no.	8	9	10	11	12	13	14	15
Fluid	HTL solids from phase separation	IHDO aqueous effluent	Aqueous effluent to APR	Gas from APR	Aq. phase from APR	Gas from APR	Gas from APR	Gas. phase from IHDO
Temperature (° C)	40,00	150,00	275,00	275	105,00	275	275	150,00
Pressure (bar-g)	1,01	30,00	30,00	30	2,00	30	30	1,01
Normal Flow Rate (Nm3/h)								
Mass Flow Rate (kg/s)	0,047	0,343	0,343	0,0032	0,340	0,0002	0,003	0,011
HHV (MJ/kg dry)	7,70	17,34	17,34	7,50	19,37	33,30	5,41	13,57
Chemical enthalpy (MW)	0,083	0,330	0,330	0,024	0,306	0,008	0,016	0,146
Thermal enthalpy (MW)	0,005	0,173	0,346	0,002	0,111	0,001	0,001	0,002
Total enthalpy (MW)	0,087	0,503	0,677	0,026	0,416	0,009	0,017	0,148
ATOMIC COMPOSITION								
Water (%wt)	77,04	94,45	94,45	0,00	95,36	0,00	0,00	0,00
Dry Matter (%wt)	22,96	5,55	5,55	100,00	4,64	100,00	100,00	100,00
Carbon, C (%wt dry)	18,60	30,64	30,64	30,00	30,77	0,00	32,43	42,52
Hydrogen, H (%wt dry)	4,88	5,26	5,26	10,00	4,28	100,00	2,70	7,37
Oxygen, O (%wt dry)	38,36	36,63	36,63	60,00	31,80	0,00	64,86	50,11
Nitrogen, N (%wt dry)	0,00	0,00	0,00	0,00	0,00	0,00	0,00	0,00
Sulfur, S (%wt dry)	0,30	1,50	1,50	0,00	1,81	0,00	0,00	0,00
Phosphorous, P (g/kg dry)	0,30	0,01	0,01	0,00	0,01	0,00	0,00	0,00
Calcium, Ca (g/kg dry)	0,00	0,00	0,00	0,00	0,00	0,00	0,00	0,00
Aluminium, Al (g/kg dry)	0,04	0,00	0,00	0,00	0,00	0,00	0,00	0,00
Iron, Fe (g/kg dry)	0,00	0,00	0,00	0,00	0,00	0,00	0,00	0,00
Magnesium, Mg (g/kg dry)	1,87	0,02	0,02	0,00	0,02	0,00	0,00	0,00
Potassium, K (g/kg dry)	39,82	49,90	49,90	0,00	60,21	0,00	0,00	0,00
Chlorine, Cl (g/kg dry)	2,02	0,57	0,57	0,00	0,69	0,00	0,00	0,00
Sodium, Na (g/kg dry)	333,89	209,22	209,22	0,00	252,45	0,00	0,00	0,00
Silicon, Si (g/kg dry)	0,13	0,00	0,00	0,00	0,00	0,00	0,00	0,00
Manganese, Mn (mg/kg dry)	542,06	15,92	15,92	0,00	19,21	0,00	0,00	0,00
SALTS COMPOSITION								
NaOH (kg / kg dry)	0,00E+00	0,00E+00	0,00E+00	0,00E+00	0,00E+00	0,00E+00	0,00E+00	0,00E+00
Na2S (kg / kg dry)	0,00E+00	0,00E+00	0,00E+00	0,00E+00	0,00E+00	0,00E+00	0,00E+00	0,00E+00
NaHS (kg / kg dry)	4,16E-03	2,11E-02	2,11E-02	0,00E+00	2,55E-02	0,00E+00	0,00E+00	0,00E+00
Na_2SO_4 (kg / kg dry)	1,91E-03	9,67E-03	9,67E-03	0,00E+00	1,17E-02	0,00E+00	0,00E+00	0,00E+00
Na_2SO_3 (kg / kg dry)	0,00E+00	0,00E+00	0,00E+00	0,00E+00	0,00E+00	0,00E+00	0,00E+00	0,00E+00
$Na_2S_2O_3$ (kg / kg dry)	3,60E-04	1,83E-03	1,83E-03	0,00E+00	2,21E-03	0,00E+00	0,00E+00	0,00E+00
Na_2CO_3 (kg / kg dry)	4,01E-04	2,03E-03	2,03E-03	0,00E+00	2,45E-03	0,00E+00	0,00E+00	0,00E+00
K_2CO_3 (kg / kg dry)	0,00E+00	0,00E+00	0,00E+00	0,00E+00	0,00E+00	0,00E+00	0,00E+00	0,00E+00

Annex C. Mass and energy flows for HTL-pulp mill integrate

This section contains the block diagrams for the reference scenario, i.e. reference pulp mill producing hardwood kraft pulp, and for the BL2F-scenarios, i.e. HTL plant integrated to pulp mill. The results are expressed as unit consumption per air dried tonne (adt) of pulp.

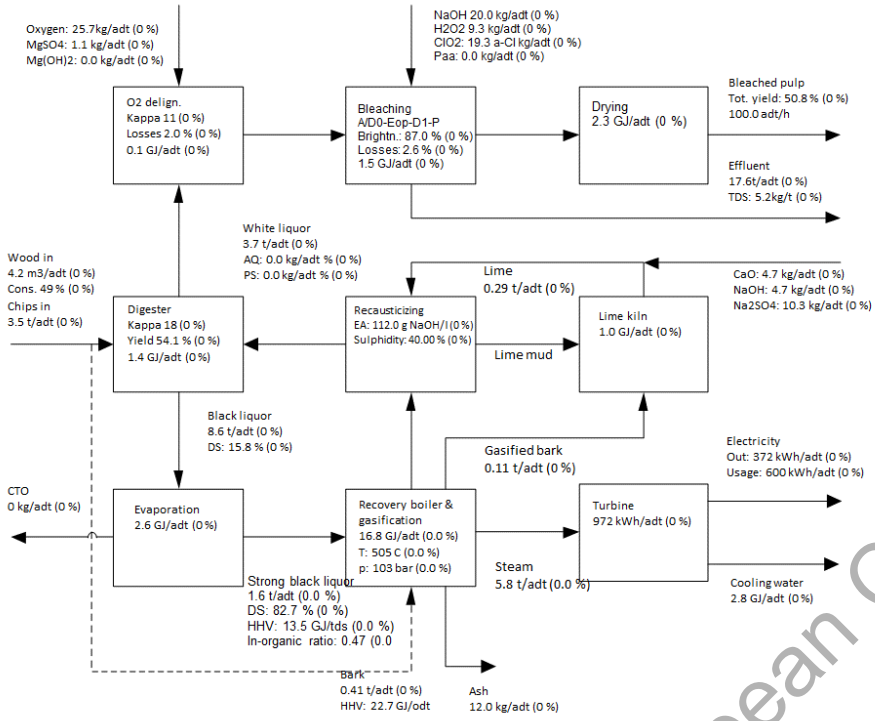

Figure 21 Block diagram for reference scenario; pulp mill producing hardwood kraft pulp, capacity 100 adt/h.

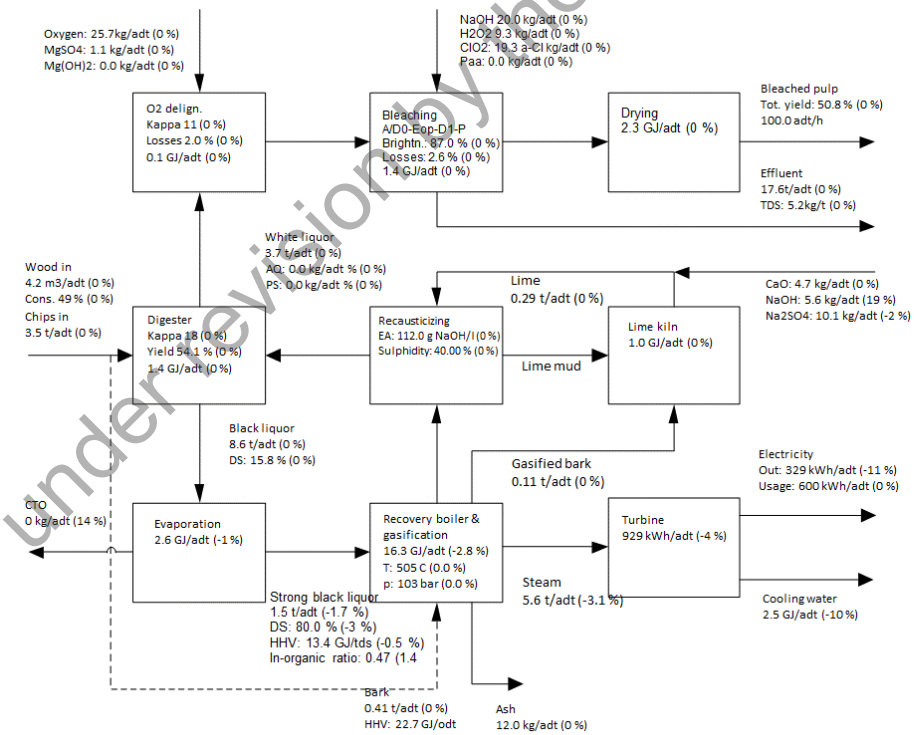

Figure 22. Block diagram for BL2F5-scenario. Differences (%) in brackets indicate when BL2F5-scenario is compared to reference scenario.

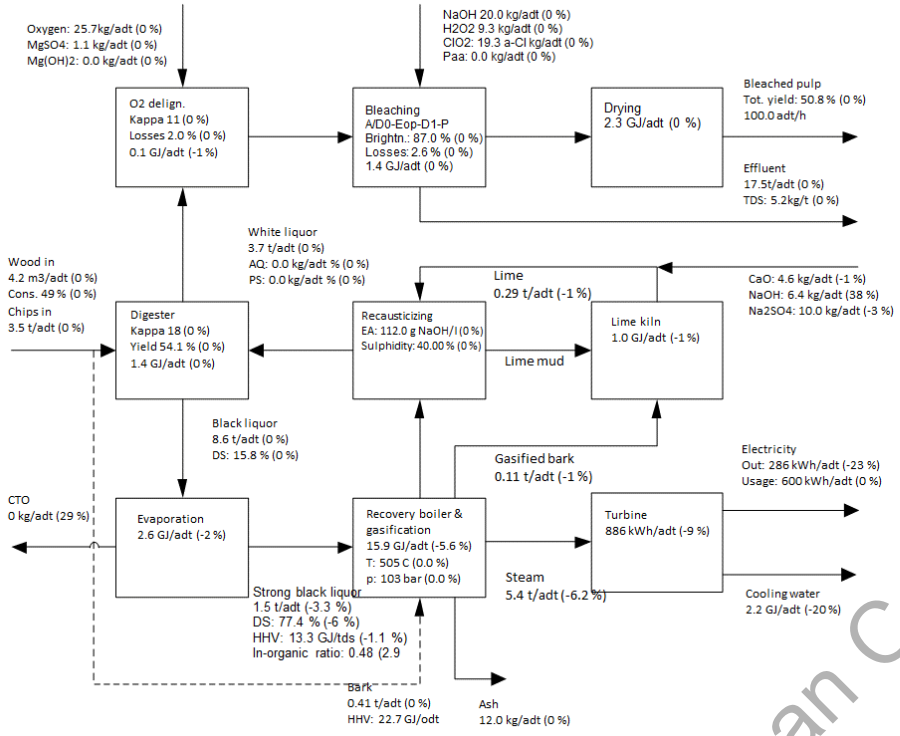

Figure 23 Block diagram for BL2F10-scenario. Differences (%) in brackets indicate when BL2F10-scenario is compared to reference scenario.

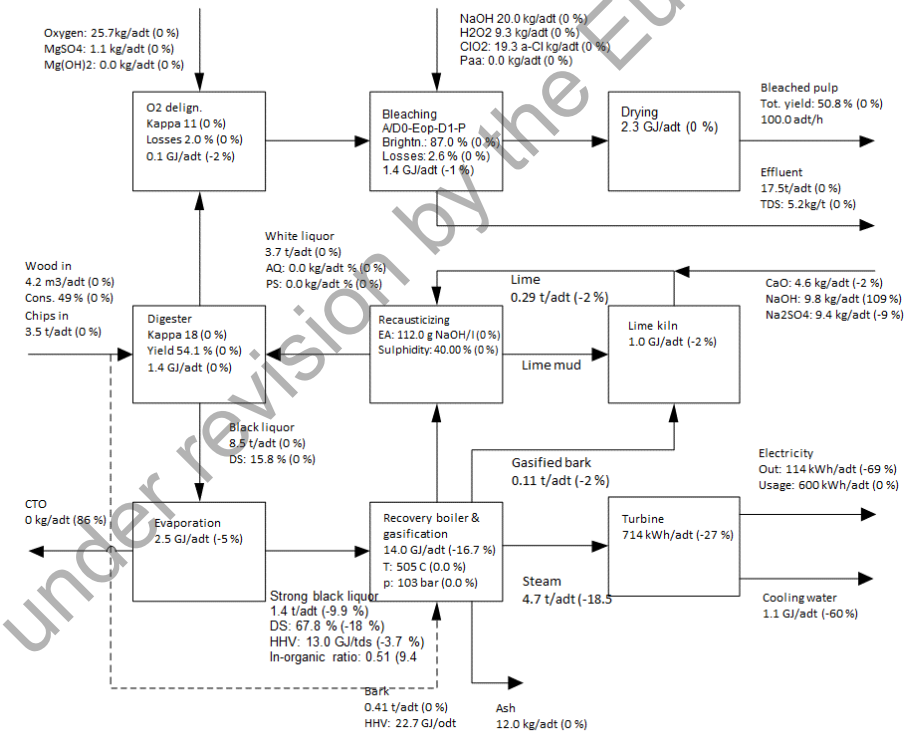

Figure 24 Block diagram for BL2F30-scenario. Differences (%) in brackets indicate when BL2F30-scenario is compared to reference scenario.

Annex D. Sodium and sulfur balances in the reference pulp mill and HTL-pulp mill integrate

This section presents the sodium and sulfur balances (kg/adt) of the pulp mill in all evaluated scenarios. The balances show only input and output streams, not the internal chemical cycle.

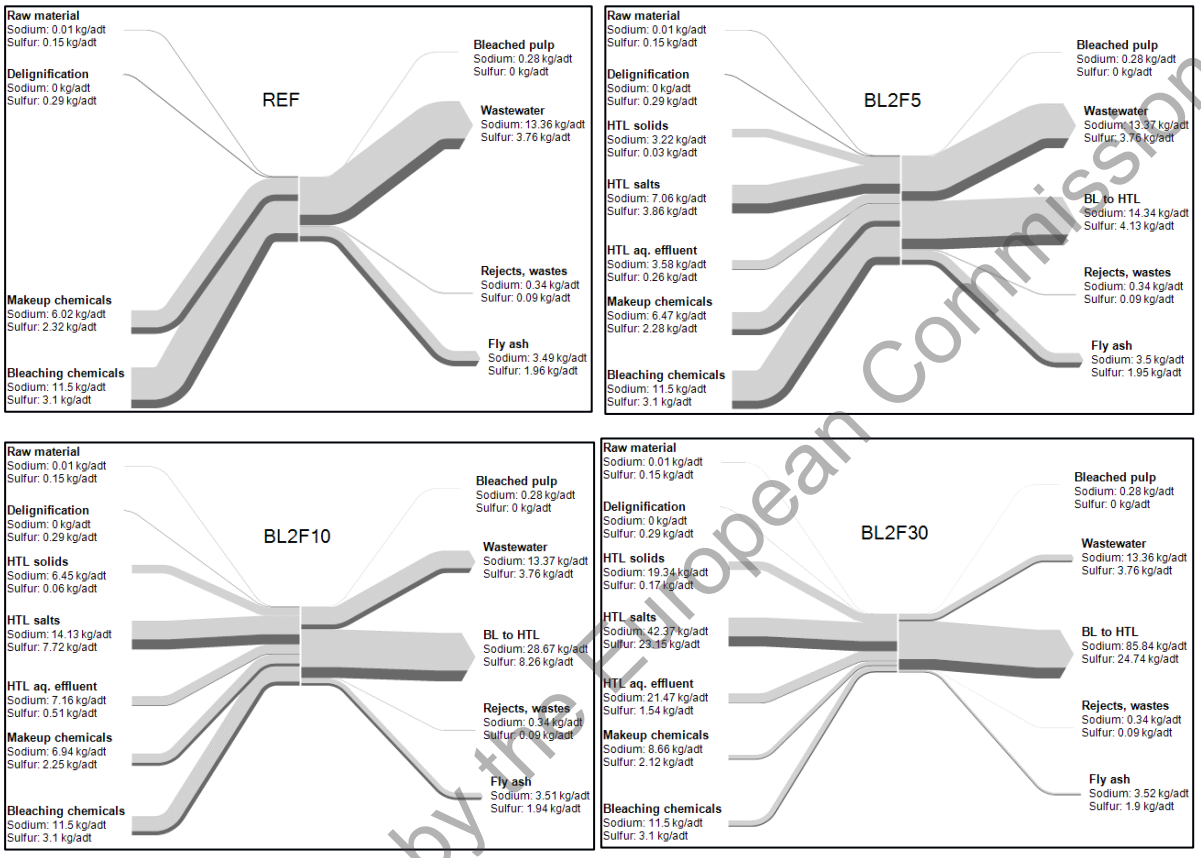

Figure 25 Sodium and sulfur balances (kg/adt) of the pulp mill in all evaluated scenarios.

Annex E. Flow calculations for the upgrading of black-liquor derived HTL-oil based on refinery processes

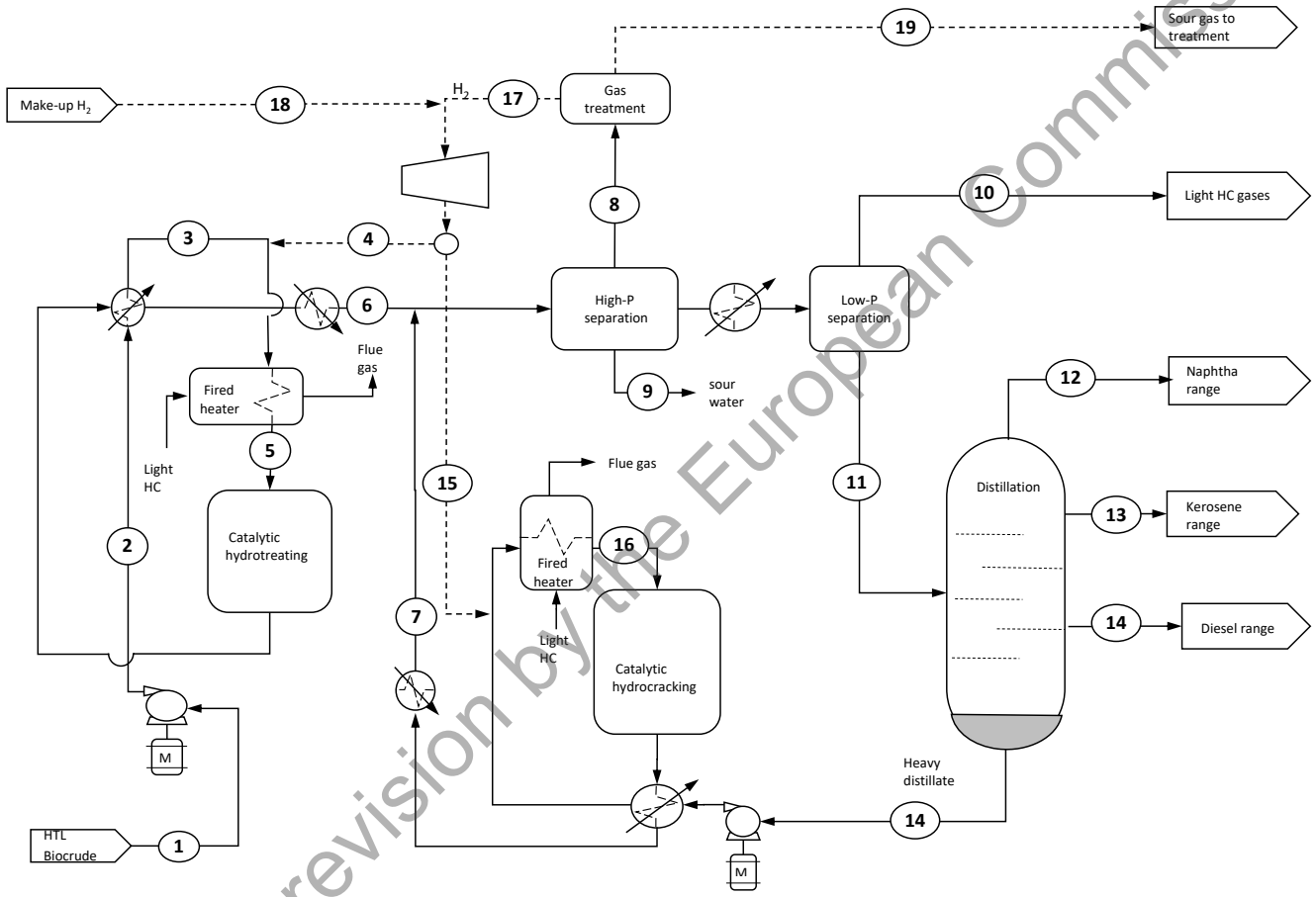

Figure 26: Mass flow diagram of the upgrading process. Numbers correspond to the stream denomination in Figure 4 and Table 18

Table 18: Preliminary calculations of the material and energy flows for the HTL plant

	Unit	1	2	2	3	4	6	7	8	9	10
		Biocrude	Pressurized Biocrude	Biocrude To HDO	H2 to HDO	Feed To HDO	HDO prod to sep	HC prod to sep	Gas to treatment	Sour Water	Light HC
Vap, Frac,		0	0	0	1	0,919	0,87	0,777	1	0	1
Temp,	*C*	40	47,1	240	360	336,9	40	40	40,1	40,1	71,5
Pressure	*kPa*	100	10000	10000	10000	10000	10000	10000	10000	10000	180
Molar Flow	*kgmole/h*	33,2	33,2	33,2	160,7	194,1	194,1	147,9	271,3	0	9,7
Mass Flow	*kg/h*	3600	3600	3600	396	3996	3996	1780	570	244	255
HHV	*MJ/kg*	39,8	39,8	39,8	118,4	47,9	47,9	48,9	115,6	44,4	44,4
Chemical Enthalpy	*MJ*	39,80	39,80	39,80	13,02	53,17	53,17	24,18	18,31	3,01	3,15
C	wt dry	0,839	0,839	0,839	0,107	0,777	0,777	0,827	0,126	0,866	0,841
H	wt dry	0,104	0,104	0,104	0,834	0,179	0,179	0,166	0,804	0,127	0,12
N	wt dry	0	0	0	0	0	0	0	0	0	0
O	wt dry	0,038	0,038	0,038	0,059	0,028	0,028	0,007	0,07	0,006	0,038
S	wt dry	0	0	0	0	0	0	0	0	0	0
Na	wt dry	0,018	0,018	0,018	0	0,016	0,016	0	0	0	0

Table 19: Preliminary calculations of the material and energy flows for the HTL plant (cont.)

	Unit	11	12	13	14	15	16	17	18	19
		Organic loquid to frac	Naphtha	Kerosene	Diesel	Heavy	H2 Crack	H2 from amine	Makeup H2	Sour gas from amine
Vap, Frac,		0,082	0	0	0	0	1	1	1	1
Temp,	*C*	39,3	134,6	225,5	285,3	377,3	360	39,2	40	46,1
Pressure	*kPa*	200	185	190	195	200	10000	241	5617	151
Molar Flow	*kgmole/h*	68	16,3	3,2	4,2	25,1	131,5	114	23,6	3
Mass Flow	*kg/h*	4845	871	725	1235	1695	85	456	47,5	114
HHV	*MJ/kg*	44,4	44,2	44,3	45,3	45,4	118,4	84,9	140,4	5,5
Chemical Enthalpy	*MJ*	59,76	10,70	8,93	15,54	21,37	2,80	10,76	1,85	0,17
C	wt dry	0,866	0,887	0,862	0,864	0,863	0,107	0,404	0	0,329
H	wt dry	0,127	0,109	0,121	0,13	0,132	0,834	0,596	1	0,021
N	wt dry	0	0	0	0	0	0	0	0	0
O	wt dry	0,006	0,004	0,017	0,006	0,005	0,059	0	0	0,651
S	wt dry	0	0	0	0	0	0	0	0	0
Na	wt dry	0	0	0	0	0	0	0	0	0